Department of Materials Science and Engineering

Experimental investigation and thermodynamic description of the BaO-containing oxide system

Rui Zhang

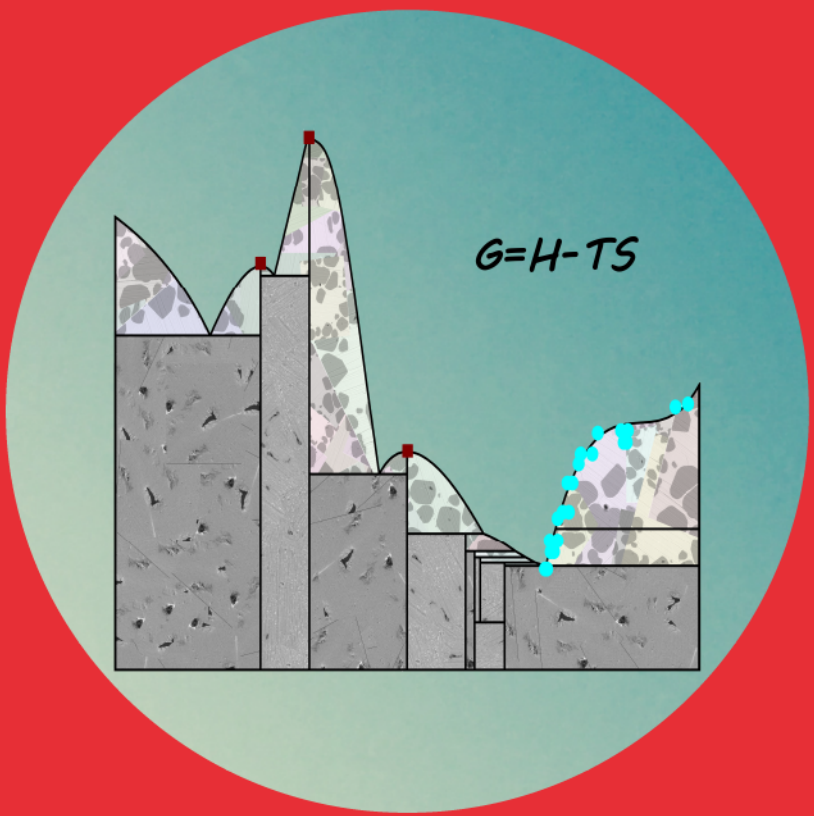

Aalto University

DOCTORAL DISSERTATIONS

Aalto University publication series
DOCTORAL DISSERTATIONS 148/2016

Experimental investigation and thermodynamic description of the BaO-containing oxide system

Rui Zhang

A doctoral dissertation completed for the degree of Doctor of Science (Technology) to be defended, with the permission of the Aalto University School of Chemical Technology, at a public examination held at the lecture hall V1 of the school on 02 September 2016 at 12.

Aalto University
School of Chemical Technology
Department of Materials Science and Engineering
Metallurgical Thermodynamics and Modelling Research Group

Supervising professor
Professor Pekka Taskinen

Thesis advisor
Professor Pekka Taskinen

Preliminary examiners
Professor Merete Tangstad, Norges Teknisk-Naturvitenskapelige Universitet, Norway
Docent Daniel Lindberg, Åbo Akademi University, Finland

Opponent
Dr. Mikko Helle, Åbo Akademi University, Finland

Aalto University publication series
DOCTORAL DISSERTATIONS 148/2016

ISBN 978-952-60-6935-7 (printed)
ISBN 978-952-60-6934-0 (pdf)
ISSN-L 1799-4934
ISSN 1799-4934 (printed)
ISSN 1799-4942 (pdf)
http://urn.fi/URN:ISBN:978-952-60-6934-0

Images: 'Phase diagram' by Rui Zhang

Unigrafia Oy
Helsinki 2016

Finland

Publication orders (printed book):
rui.2.zhang@aalto.fi

441 697
Printed matter

Aalto University

Abstract

Aalto University, P.O. Box 11000, FI-00076 Aalto www.aalto.fi

Author
Rui Zhang

Name of the doctoral dissertation
Experimental investigation and thermodynamic description of the BaO-containing oxide system

Publisher School of Chemical Technology

Unit Department of Materials Science and Engineering

Series Aalto University publication series DOCTORAL DISSERTATIONS 148/2016

Field of research Metallurgy

Manuscript submitted 14 April 2016 **Date of the defence** 2 September 2016

Permission to publish granted (date) 28 June 2016 **Language** English

☐ **Monograph** ☒ **Article dissertation** ☐ **Essay dissertation**

Abstract

A thermodynamic description of the metallurgical and ceramic system is beneficial when predicting the phase equilibria, thermodynamic properties and other significant properties. The mathematical expression of Gibbs energy has been adopted to realize the thermodynamic description of the systems. Employing the CALPHAD technique, the thermodynamic parameters in the Gibbs energy functions of various phases in the systems can be optimized by fitting with the experimental data available. The thermodynamic assessment of the unary and binary systems plays a fundamental role in the establishment of the thermodynamic database, because the accuracy of the unary and binary data largely determines the reliability of the extrapolation into higher order systems.

In the present thesis, experiments were conducted to study the phase equilibria in the BaO-MgO, BaO-Al_2O_3 and BaO-SiO_2 systems. For the BaO-Al_2O_3 and BaO-SiO_2 systems, the liquidus was constructed using a high temperature equilibration/quenching/EPMA technique. The phase stability and phase relations (below 1523 K) in the BaO-MgO, BaO-Al_2O_3 and BaO-SiO_2 systems were identified by XRD and SEM/EDS. The literature data combined with the personal experiments were evaluated for thermodynamic modelling.

Thermodynamic assessment was performed by means of the CALPHAD technique for the BaO-SrO, BaO-CaO, BaO-MgO, BaO-Al_2O_3, BaO-SiO_2 and SrO-SiO_2 systems. For the BaO-SrO, BaO-CaO and BaO-MgO systems, substitutional solution model was adopted to express the molten phase. For the BaO-Al_2O_3, BaO-SiO_2 and SrO-SiO_2 systems, associate solution model with one associate was applied to describe the molten phase. Moreover, two associates, Ba_2SiO_4 and $BaSiO_3$, were tested to model the liquid behaviour in the BaO-SiO_2 system. The calculated phase diagrams and thermodynamic properties were compared with experimental data. Sets of consistent thermodynamic parameters were presented for the assessed oxide systems.

The isothermal section of the BaO-Al_2O_3-SiO_2 ternary system at 1773 K was determined by an equilibration/quenching technique and SEM/EDS. On the basis of the MTOX oxide database, the isothermal sections of this ternary system at 1673 K, 1773 K, 1873 K and 1973 K were calculated.

Keywords Phase equilibrium, Thermochemical properties, CALPHAD, Thermodynamic assessment, BaO

ISBN (printed) 978-952-60-6935-7 **ISBN (pdf)** 978-952-60-6934-0

ISSN-L 1799-4934 **ISSN (printed)** 1799-4934 **ISSN (pdf)** 1799-4942

Location of publisher Helsinki **Location of printing** Helsinki **Year** 2016

Pages 118 **urn** http://urn.fi/URN:ISBN:978-952-60-6934-0

Preface

The research work of the present doctoral thesis was conducted at Aalto University, School of Chemical Technology, Metallurgical Thermodynamics and Modelling Research Group during the years 2013 – 2016. Firstly, I would like to express my deepest appreciation to my supervisor, Professor Pekka Taskinen. It is him who offered me the opportunity to pursue my dream in academia when I was in the darkest period of my life. I am greatly impressed by his depth of knowledge that every time my problem could be solved after discussing with him. He deserves my utmost respect not only because of his profession but of his action by creating a free atmosphere for critical thinking. It is my privilege to have you as my supervisor for doctoral study and work.

Secondly, I would like to thank Professor Malin Selleby and Dr. Huahai Mao from KTH Royal Institute of Technology for their enthusiastical supports of my study. I will never forget the detailed instructions from Huahai about how to fix the problems in thermodynamic assessment. When I started my academic career in Finland in the year 2013, the encouragement from Professor Guven Akdogan was of great value.

I owe a debt of gratitude to my dear colleagues, Joseph Hamuyuni, Dmitry Sukhomlinov, Petteri Halli, Markus Aspiala, Niko Hellstén and Imam Santoso. Without their help, it is impossible to establish the setup for experiments. I would like to thank Katri Avarmaa for being my officemate and critically proof-reading my thesis. The appreciation should also be given to Longgong Xia (shidi) for being my roommate and joking about lives here. Thank you, Dr. Pia Lapalainen, for reviewing my 'introduction'.

Hanna Viitala, Petteri Piskunen and Lassi Klemettinen are acknowledged for the SEM tutorial lecture and analysis. I will always remember the interesting talk and stories with Hanna during SEM analysis. The acknowledgement should also be given to Lassi Pakkanen from the Geological Survey of Finland (GTK) for EPMA analysis.

I am grateful to CIMO (Centre for International Mobility, Finland) for financing me to work in Pekka's group for half a year in 2013. I appreciate the grants from STT foundation (Stiftelsen för Tillämpad Termodynamik, Sweden) for attending the summer school in France, 2014 and the CALPHAD conference in Italy, 2015. The Larry Kaufman grant from CALPHAD committee and the travel grant from FinCEAL Plus are appreciated for providing me the opportunity to attend the CALPHAD conference in Japan, 2016. The research throughout the my doctoral study was financially supported by Association of

Finnish Steel and Metal Producers, Tekes and System Integrated Metal Processes (SIMP) program by FIMECC.

The happy time with my friends from Helsinki University is unforgettable: the hotpot, the card games and the birthday party with a big surprise.

The love from my parents made it possible to finalize my doctoral study. I know how hard it is to live far away from them. They always support my decision without any reservation.

Finland is a magic country. I found my love here. Lei Zhao, I promise I will live the rest of my life with you.

Espoo, 7 April 2016
Rui Zhang

Contents

List of Abbreviations and Symbols

Abbreviations

BSE	Backscattered Electrons
CALPHAD	CALculation of PHAse Diagram
CEF	Compound Energy Formalism
DSC	Differential Scanning Calorimetry
DTA	Differential Thermal Analysis
EMF	Electromotive Force
EPMA	Electron Probe Micro-Analysis
EXP	Experimental data file used in Thermo-Calc software
FactSage	Thermochemical software and database
ICME	Integrated Computational Materials Engineering
LTCCs	Low Temperature Co-fired Ceramics
LRO	Long-Range Order
MTDATA	Thermochemical software from National Physical Laboratory
MTOX	Metal-oxide-sulphide-fluoride thermodynamic database
MQM	Modified Quasichemical Model
MACRO	A quick calculation of various diagrams in Thermo-Calc
PARROT	A module in Thermo-Calc used for parameter optimization
PANDAT	Thermochemical computational software
POP	Experimental data storage file used in Thermo-Calc
SOFCs	Solid Oxide Fuel Cells
SGTE	Scientific Group Thermodata Europe
SEM/EDS	Scanning Electron Microscope/Energy Dispersive X-ray Analysis

SETUP	Storage of models and parameters in Thermo-Calc
SRO	Short-Range Order
Thermo-Calc	Thermodynamic software
TGA	Thermogravity Analysis
XRD	X-ray Powder Diffraction

Symbols

C_p	heat capacity
G	Gibbs energy
${}^{srf}G_m$	Gibbs energy of unreacted mixture of the constituents of a phase
${}^{phys}G_m$	physical contribution to the Gibbs energy
${}^{E}G_m$	excess Gibbs energy
H	enthalpy
H_i^{SER}	enthalpy of the element i in its reference states
L	interaction parameter
P	pressure
R	gas constant
S	entropy
${}^{conf}S_m$	configurational entropy of a phase
T	temperature
μ	chemical potential
α	thermal expansion

Superscripts and subscripts

$conf$	configurational
E	excess
i, j, k	element or component
m,n	order of the polynomial
m	molar
o	standard state

phys	physical
SER	Standard Element Reference states at 298.15 K and 1 bar
srf	surface of reference
θ,φ	a phase

List of Publications

This doctoral dissertation consists of a compendium and the following publications which are referred to in the text by Roman numerals.

Publication I. Zhang, Rui; Taskinen, Pekka. 2015. Experimental investigation and thermodynamic modelling of the BaO-MgO system. Proceedings of European Metallurgical Conference 2015 (EMC). Düsseldorf, June 14-17. Volume 1. 443-452. ISBN 978-3-940276-61-2.

Publication II. Zhang, Rui; Taskinen, Pekka. 2015. A phase equilibria study and thermodynamic assessment of the $BaO\text{-}Al_2O_3$ system. CALPHAD, 51, 42-50. DOI: 10.1016/j.calpahd.2015. 07.003.

Publication III. Zhang, Rui; Taskinen, Pekka. 2016. Experimental investigation of liquidus and phase stability in the $BaO\text{-}SiO_2$ binary system. Journal of Alloys and Compounds, 657, 770-776. DOI: 10.1016/j.jallcom.2015.10.165.

Publication IV. Zhang, Rui; Mao, Huahai; Halli, Petteri; Taskinen, Pekka. 2016. Experimental phase stability investigation of compounds and thermodynamic assessment of the $BaO\text{-}SiO_2$ binary system. Journal of Materials Science, 51, 10, 4984-4995. DOI: 10.1007/S10853-016-9803-0.

Publication V. Zhang, Rui; Mao, Huahai; Taskinen, Pekka. 2016. Thermodynamic descriptions of the BaO-CaO, BaO-SrO, $BaO\text{-}SiO_2$ and $SrO\text{-}SiO_2$ systems. CALPHAD, 54, 107-116. DOI: 10.1016/j.calphad.2016.06.009.

Author's Contribution

Publication I. Experimental investigation and thermodynamic modelling of the BaO-MgO system

The phase equilibria of the BaO-MgO system was studied by the author based on the self-planned equilibration-quenching experiments and results of SEM/EDS analysis. The experimental set-up was established with assistance of colleagues. A critical literature review was made by the author. Based on the literature data, the thermodynamic assessment was performed using Thermo-Calc by the author and a set of self-consistent thermodynamic parameters were achieved. The author prepared the manuscript with input from the co-author.

Publication II. A phase equilibria study and thermodynamic assessment of the $BaO\text{-}Al_2O_3$ system

The liquidus in equilibrium with phase $BaAl_2O_4$ and the eutectic reaction, liquid $\rightarrow BaAl_2O_4 + Ba_3Al_2O_6$, in the $BaO\text{-}Al_2O_3$ were investigated by the author, based on the self-planned equilibration-quenching experiments and SEM/EDS and EPMA analysis. The phase relations in the BaO-rich region was experimentally studied by the author based on the results of XRD. A critical literature survey was made by the author, focusing on the phase diagram and thermodynamic properties of the $BaO\text{-}Al_2O_3$ system. By using associate solution model and substitutional solution model for the description of the liquid phase, a thermodynamic assessment was performed by the author using Thermo-Calc. The technical problems during assessment were solved with the help of Dr. Huahai Mao and Dr. Olga Fabrichnaya. According to the thermodynamic parameters obtained by the author, an improved phase diagram and thermodynamic properties of this system were presented. The author prepared the manuscript with the input from the co-author.

Publication III. Experimental investigation of liquidus and phase stability in the $BaO\text{-}SiO_2$ binary system

A critical literature review was made by the author. The liquidus of the $BaO\text{-}SiO_2$ system in the SiO_2-rich corner was experimentally constructed by the author using an equilibration-quenching technique and SEM/EDS and EMPA analysis. The author determined the phase relations of the stoichiometric compounds in the high-baria regions by XRD. The phase diagram of the $BaO\text{-}SiO_2$ system was calculated by the author based on the MTOX oxide database, compared with the present experimental data and literature data. The author prepared the manuscript with the input from the co-author.

Publication IV. Experimental phase stability investigation of compounds and thermodynamic assessment of the $BaO\text{-}SiO_2$ binary system

The author determined the phase equilibria of the $BaO\text{-}SiO_2$ system in the BaO-rich region at 1173 K and 1523 K, based on the self-planned experiments and XRD results. The set-up of the experiments was established with the help of colleagues. By using associate solution model and substitutional solution model to describe the liquid phase, the thermodynamic assessment was performed by the author and co-author using Thermo-Calc. A set of thermodynamic parameters capable of describing the $BaO\text{-}SiO_2$ system was achieved. The author prepared the manuscript with the input from the co-authors.

Publication V. Thermodynamic descriptions of the BaO-CaO, BaO-SrO, $BaO\text{-}SiO_2$ and $SrO\text{-}SiO_2$ systems

A critical literature review was made by the author. By using substitutional solution model to describe the liquid phase, the BaO-CaO and BaO-SrO systems were thermodynamically assessed by the author. The thermodynamic assessment was conducted by the author regarding the $BaO\text{-}SiO_2$ and $SrO\text{-}SiO_2$ systems, by using associate solution model for the description of the liquid phase. For the $BaO\text{-}SiO_2$ system, two associates, Ba_2SiO_4 and $BaSiO_3$, were employed to test the feasibility and validity to describe the $BaO\text{-}SiO_2$ system. The author prepared the manuscript with the input from the co-authors.

1. Introduction

1.1 Research background

BaO-SrO-CaO-MgO-Al_2O_3-SiO_2 system has drawn tremendous attentions due to its wide applications in metallurgy, glass ceramics and geochemistry. The materials containing this multi-component oxide system are extraordinarily difficult to investigate because of high experimental temperature, long equilibration and diffusion time and corrosive impact. This has led to the absence of systematic knowledge on the phase equilibrium, thermodynamic properties and microstructure, which largely determine the properties of the final products in industrial applications.

Oxide slag is normally applied to remove sulphur in steelmaking [1,2], however, the capability of removing impurities is limited unless a highly basic oxide is added to the flux. BaO-CaO-MgO-Al_2O_3-SiO_2 system, as the basis of the BaO-containing oxide slag, is poorly investigated by experiments despite the high popularity of its desulfurization ability compared with lime-based slags [3-5]. On the basis of BaO-SrO-CaO-MgO system, with addition of Al_2O_3, SiO_2 and B_2O_3 of various compositions, a series of glass ceramics can be prepared to be used for (i) joining or sealing both tubular and planar ceramic solid oxide fuel cells (SOFCs) [6-8] and (ii) producing low temperature cofired ceramics (LTCCs) for advanced electronic packages [9-11]. Complex chemical reactions and variations of thermodynamic properties taking place during the preparation of the glass ceramics are essential for the understanding of the microstructure and dielectric properties. Consequently, a good knowledge of the phase equilibria and thermodynamic properties is necessary to efficiently investigate the technical process and materials preparation regarding the BaO-SrO-CaO-MgO-Al_2O_3-SiO_2 system.

With the advent [12-14] and advanced development of the CALPHAD (CALculation of PHAse Diagram) technique, it is now possible to establish a complete and accurate thermodynamic database capable of describing the complex oxide systems. The thermodynamic database is utilized to model and predict the phase equilibria, thermodynamic properties and chemical processes of the desired systems. Generally, two factors determining the accuracy and reliability of the thermodynamic database are regarded as (i) experimental data employed for thermodynamic assessment and optimization and (ii) thermodynamic models. Thermodynamic parameters in the database should be assessed and optimized using experimental data available since most of the measurements are quantitatively related to the thermodynamic functions [15].

So the availability and accuracy of the experimental measurements have a great impact on the quality of the final thermodynamic parameters in the database. On the other hand, the thermodynamic models are employed to express the thermodynamic properties of phases in the system, where the description of the liquid phase across the full compositional range is a key part. For the oxide system, the ideal condition is to model the liquid phase based on the distribution and mixing properties of the actual species in the solution. However, the knowledge of the mixing behaviour and physical properties of the oxide melts is narrow, making it unable to fulfil the ideal condition. An alternative to model the liquid phase is to concentrate on the measured thermodynamic properties of the solution phase although the model is hard to be physically interpreted. Several models were developed by considering this problem, for example, the ionic two-sublattice liquid model by Hillert et al. [16] and Sundman [17], modified quasi-chemical model by Lin and Pelton [18] and so on, associate solution model by Sommer [19] and Krull et al. [20], cell model by Kapoor and Frohberg [21], and Margules solution model by Berman and Brown [22]. By using associate solution model, there is an increasing number of reports that well reproduce the experimental data. So the validity and feasibility of this model employed on the oxide systems in the present work are worth testing.

With the assistance of computer and software, thermodynamic calculation, assessment and optimization can be realized efficiently. The PARROT module in the Thermo-Calc software package [23] possesses a high reputation for its parameter optimization function. The MTOX oxide database [24] in the MTDATA software [25] utilizes the associate solution model for the description of the molten phase in the oxide systems. Consequently, Thermo-Calc [23] and MTDATA [25] were selected as the tool in the present work for thermodynamic optimization and calculation.

1.2 Objectives and structure of the thesis

The present thesis aimed at:

1. acquiring data of the liquid phase equilibria and phase relations of the stoichiometric compounds in the BaO-MgO, BaO-Al_2O_3, BaO-SiO_2 and BaO-Al_2O_3-SiO_2 systems;
2. performing thermodynamic assessment of the BaO-CaO, BaO-SrO, BaO-MgO, BaO-Al_2O_3, BaO-SiO_2 and SrO-SiO_2 systems;
3. testing the validity of associate solution model for the description of the molten phase in the BaO-Al_2O_3, BaO-SiO_2 and SrO-SiO_2 systems;
4. calculating the phase diagrams and thermodynamic property diagrams based on the thermodynamic parameters obtained in the present work, and comparing them with the experimental data available.

Although the experimental investigations on the oxide systems studied in the present work can be traced to the early 20th, large discrepancies are frequently observed in the available literature data. New and more accurate experimental measurements are necessary in order to improve the knowledge of the desired oxide systems. Equilibration-quenching technique combined with direct phase

analysis approach is widely employed to construct the liquidus and phase relations of the phase diagram. With the experimental data obtained in the present work and in the literature, the thermodynamic parameters for various phases in the oxide systems were optimized by using Thermo-Calc.

The present thesis contains one peer-reviewed conference publication [I], four peer-reviewed journal publications [II-V] and the present compendium. The publications are attached in the Appendices.

2. The CALPHAD method

Phase diagram is a graphical representation of a substance at an equilibrium state to show the conditions (temperature, pressure and concentration) under which different phases coexist. It can be used as a significant tool among the metallurgists, ceramists, and earth and materials scientists to study phase transformation, alloy preparation and to achieve thermodynamic properties. Generally, the phase diagrams we use are for binary and ternary systems. However, practically, most systems in nature and industry contain multi-components, which, to some extents, bring about some difficulties for investigation. Employing the CALPHAD (CALculation of PHAse Diagrams) approach, it can help to study the phase diagrams of multi-components system by extrapolating the binary or ternary systems into higher-order systems. The CALPHAD method can be well understood as 'The Computer Coupling of Phase Diagrams and Thermochemistry' [26]. It aims at obtaining a set of thermodynamic descriptions of a system on the basis of critical evaluation of the available experimental data, so that the database of the multi-components system can be established. In 1970, the description of the CALPHAD method and the computer program packages were presented by Kaufman and Bernstein [27]. With the assistance of computers, the whole process is time-saving and efficient, compared with the previous manual work. By using the CALPHAD method, each phase of the system is expressed by a Gibbs energy function, which will be introduced in the next chapter. The thermodynamic parameters of the Gibbs energy function are assessed and optimized by coupling the phase diagram and thermochemical data. The procedure of the CALPHAD method is shown in Figure 1.

The start of the CALPHAD approach is from the collection of the available experimental data, for example, phase equilibria data, thermodynamic data (heat capacities, enthalpies of formation, enthalpies of mixing and activities etc.) and electromotive force data. In recent years, with the development of the first principle calculation, the calculated total energy can be employed as experimental data. The accuracy and reliability of the available experimental data should be evaluated based on the experimental techniques used and how they are introduced [15]. By considering the time and capital cost of experiments, all the available data should be considered by giving different weights during the assessment. Further experiments are recommended to bridge the gap where scarce data can be acquired. After collecting and evaluating the experimental data, each phase of the system is physically

modelled by a Gibbs energy function with respect to temperature, composition and pressure. The choice of thermodynamic model should have physical and chemical sound and adequate for the P-T-x domain of phase stability [28]. The detailed description of the thermodynamic models is provided in the next chapter. By weighted nonlinear least square analysis [23], the model parameters are optimized by fitting to the experimental data. Currently, the commercial software packages, including Thermo-Calc [23], MTDATA [25], Pandat [29] and FactSage [30] are mostly used for performing the thermodynamic assessment and optimization. Thermo-Calc [23] was employed throughout the present work because of its powerful function for global Gibbs energy minimization and its user-friendly interface. It is wise to perform the calculation of phase diagram and thermodynamic properties and compare the calculated results with the experimental data, in order to abandon or adjust weights of the experimental data, which are found difficult to fit. As is shown in Figure 1, it should be kept in mind that the backward repetition of various processes is needed to re-evaluate the experimental data, adjust the parameters or even modify the thermodynamic model. It is hard to draw the conclusion that the best set of optimized thermodynamic parameters has been acquired. As a rule, a well-optimized set of parameters for the Gibbs energies of the system should be able to reproduce the available experimental set in the best possible manner [15].

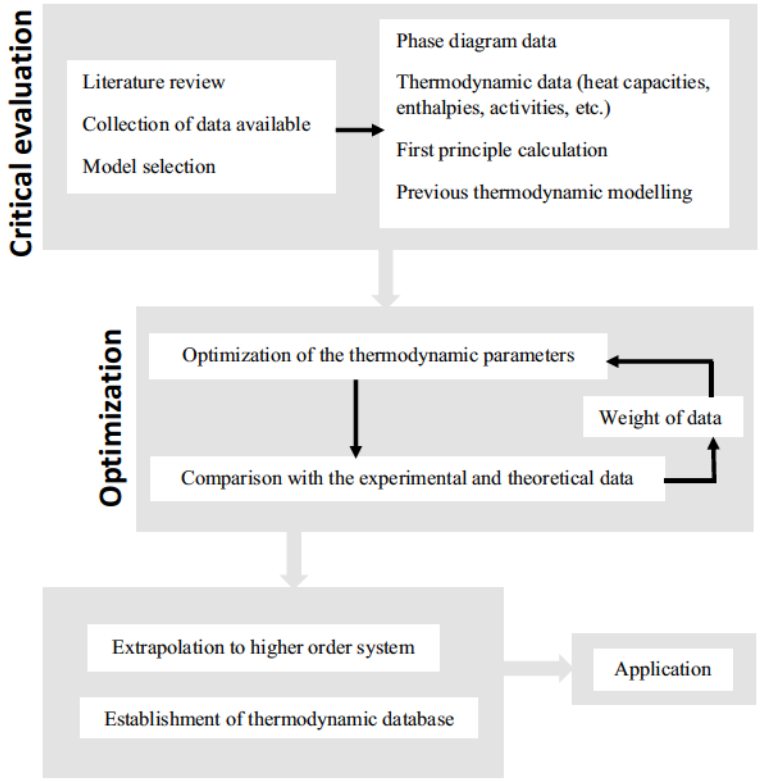

Figure 1. The flowchart of the CALPHAD method.

To construct multi-component thermodynamic database is one of the major targets of the CALPHAD method. The well-developed thermodynamic database can be widely applied in steelmaking, extractive metallurgy, and slag refining for nuclear waste disposal and so on. Multi-components systems are always involved in the practical applications. Accurate and reliable description of the unary and binary system is regarded as the foundation to make a good extrapolation into higher orders. Consequently, it is of great significance to describe the unary and binary systems in a systematic and scientific means.

In recent years, for the subject of materials design, CALPHAD method has been combined with the first principle calculation (density functional theory) [30] and kinetics calculation (diffusion databases) [31] for microstructure simulation and performance prediction. Based on the combination of various techniques, the emerging ICME (Integrated Computational Materials Engineering) approach has been raised [32-36]. It contributes to design and optimize new materials adopting integrated simulation tools. Further improvements are required focusing on (i) the developments of thermodynamic and mobility databases, (ii) simplifying the structure models and shortening the time for microstructure simulation (phase field and Monte Carlo) and (iii) interdisciplinary cooperation to conquer industrial barriers.

3. Thermodynamic modelling

Thermodynamic modelling plays an indispensable role in the CALPHAD approach as it determines the quality of the optimization and thermodynamic parameters acquired. In the CALPHAD method, the Gibbs energy (G) is applied as the modelled thermodynamic property, due to the fact that Gibbs energy is a function of temperature (T) and pressure (P), which are the conditions that most experiments and industrial process are conducted. In ambient environment, the contribution of pressure to Gibbs energy can be ignored. From the Gibbs energy all other important thermodynamic quantities can be derived, for example, heat capacity (C_p), enthalpy (H), entropy (S), chemical potential (μ), and thermal expansion (α).

3.1 General form of the Gibbs energy

Thermodynamic models should be able to represent the physical and thermochemical properties of materials with a small number of thermodynamic parameters.

The general form of the total Gibbs energy of a phase is expressed as:

$$G_m = {}^{srf}G_m + {}^{phys}G_m - T \cdot {}^{conf}S_m + {}^{E}G_m \quad (1)$$

where the superscript '*srf*' stands for 'surface of reference' and the '*phys*' represents the physical contribution to the Gibbs energy such as magnetic transitions. The configurational entropy of the phase is denoted as, ${}^{conf}S_m$. The term, ${}^{E}G_m$, stands for the excess Gibbs energy, describing the remaining part from the real Gibbs energy [15].

As introduced above, the temperature dependent Gibbs energy for a phase with fixed composition is widely accepted. So in the following text and the present assessment work, the Gibbs energy function with respect to temperature is employed. The temperature dependence of the molar Gibbs energy for a stable component in a phase θ is usually described by the polynomial as:

$$G_m^{\theta} - \sum_i b_i H_i^{SER} = a_0 + a_1 T + a_2 T ln(T) + a_3 T^2 + a_4 T^{-1} + a_5 T^3 + \cdots \quad (2)$$

where b_i is the stoichiometry of element i in θ and $\sum_i b_i H_i^{SER}$ stands for the sum of the enthalpies of the elements in their reference states (at 298.15 K and 1 bar, Stable Element Reference, denoted as SER). Since the absolute value of the

enthalpy of a system is unavailable, the term $\sum_i b_i H_i^{SER}$ is required and a reference state should be selected. T is the absolute temperature. The other temperature dependent terms can be used and the functions can be split in several temperature intervals. It should be noted that the equation (2) is used from 298.15 K upwards, as in the Gibbs energies by SGTE (Scientific Group Thermodata Europe). For most cases, the lower temperature limit of 298.15 K is sufficient to allow the calculations of equilibrium in heterogeneous systems where diffusion is needed to reach the equilibrium state [15]. However, diffusion at this low temperature is so difficult that extending the thermodynamic model at and below 298.15 K is of less practical interest. The coefficients, a_0, a_1, a_2..., are temperature dependent, which are to be optimized by fitting the experimental and theoretical data using least-square method to minimize the global Gibbs energy of the whole system. After mathematical calculations, these coefficients are related with thermodynamic quantities which can be measured and calculated,

$$H_m^\theta - \sum_i b_i H_i^{SER} = a_0 - a_2 T - a_3 T^2 + 2a_4 T^{-1} - 2a_5 T^3 \cdots \quad (3)$$

$$S_m^\theta = -a_1 - a_2[1 + \ln(T)] - 2a_3 T + a_4 T^{-2} - 3a_5 T^2 \cdots \quad (4)$$

$$C_p^\theta = -a_2 - 2a_3 T - 2a_4 T^{-2} - 6a_5 T^2 \cdots \quad (5)$$

The coefficients in equations (3-5) are the same as those in equation (2). When the heat capacity data and enthalpy data are available at high temperature, the linear and quadratic terms can be used for thermodynamic optimization, or else it may give rise to large errors when the low temperature is extrapolated to high temperature.

3.1.1 Unary oxides

The Gibbs energy of component o in phase φ, ${}^{o}G_o^\varphi = G_o^\varphi(T) - \Sigma H_i^{SER}$, (o=BaO, SrO, CaO, MgO, Al_2O_3 and SiO_2, and i=Ba, Sr, Mg, Ca, Al, Si and O) is expressed by the polynomials:

$$G_o^\varphi(T) = a + bT + cT\ln T + dT^2 + eT^{-1} + fT^3 + gT^7 + hT^{-9} \quad (6)$$

ΣH_i^{SER} is the sum of enthalpies of the elements at 298.15 K and 1 bar in their stable states.

In the present work, the BaO-containing oxide system (SrO, CaO, MgO, Al_2O_3 and SiO_2) was studied. The choice of the thermodynamic parameters for BaO was the preliminary task to ensure the reliability of the following thermodynamic calculations. After critical literature evaluation and comparison (shown in the Chapter 'Results and discussion'), the Gibbs energy functions for pure BaO are consistent with SGTE94 [37]. The thermodynamic databases for pure CaO, MgO, Al_2O_3 and SiO_2 are directly taken from well assessed thermodynamic parameters by Mao et al. [38,39] and Hallstedt [40,41], and the thermodynamic description of SrO is from SGTE94 [37].

3.1.2 Solution phases

Oxide melts can be considered as an essential part of thermodynamic modelling in the full range of compositions and as strongly ordered substances. Many models are applicable to describe the oxide systems and other ionic systems, as mentioned in the 'introduction'. They are substitutional model, the ionic two-sublattice liquid model by Hillert et al. [16] and Sundman [17], modified quasi-chemical model by Lin and Pelton [18] and so on, associate solution model by Sommer [19] and Krull et al. [20], cell model by Kapoor and Frohberg [21], and Margules solution model by Berman and Brown [22].

Substitutional solution model is employed for phases such as gas phase or simple solutions where components can mix on any spatial position [26]. It can be regarded as the simplest model to describe the thermodynamic behaviour of the solution phase. When there is no term of excess Gibbs energy, the model is named as ideal substitutional solution model. It is not recommended to apply the substitutional solution model to describe the solutions with strong ordering [28]. When the interactions between the components in the system show the behaviour of long range order (LRO), the substitutional model can be modified to sub-lattice model, according to the Compound Energy Formalism (CEF) [42,43]. When the solutions exhibit short range order (SRO), associates can be introduced, which is named as associate solution model.

The Gibbs energy described using substitutional solution model is given by:

$$G_m = \sum_{i=1}^{n} x_i \, {}^{o}G_i + RT \sum_{i=1}^{n} x_i \ln(x_i) + {}^{E}G_m \qquad (7)$$

where ${}^{o}G_i$ denotes the Gibbs energy of the phase containing the pure component i. x_i is the mole fraction of the component i. ${}^{E}G_m$ is the excess Gibbs energy of binary interaction, which can be expressed using Redlich-Kister polynomials [44] as follows:

$${}^{E}G_m = x_i x_j \sum_{n=0}^{m} {}^{n}L_{ij}(x_i - x_j)^n \qquad (8)$$

where ${}^{n}L_{ij}$ is the interaction parameter of different species to be optimized in the present work. The general temperature dependent form, ${}^{n}L_{ij}$=a+b*T, was adopted.

As mentioned above, if the liquid phase tends to show a strong short range order, the term 'associate' expresses an interaction of the 'associate' with different components in the system. The associate solution model employs associate(s) as a constituent in the solution for thermodynamic modelling. Then the thermodynamic properties of the liquid phase depend predominantly on the Gibbs energy formation of the associates instead of the interactions between the components [26]. Therefore, the diagram of enthalpy of mixing in liquid should show a V-shape at the stoichiometry of the associates, and thus the configurational entropy is low at that composition. The associate solution model is applied to describe the solution phases in the systems BaO-Al_2O_3, BaO-SiO_2 and SrO-SiO_2.

By using associate model to describe a binary A-B system, the molten phase is assumed to be constituted of three species: A, A_aB_b, B. The molar Gibbs energy function of the molten phase can be expressed as:

$$G_m^{Liq} - \sum H_i^{SER} = y_A \, {}^oG_A^{Liq} + y_B \, {}^oG_B^{Liq} + y_{A_aB_b} \, {}^oG_{A_aB_b}^{Liq}$$

$$+RT\left(y_A ln y_A + y_A ln y_A + y_{A_aB_b} ln y_{A_aB_b}\right) + {}^EG_m \quad (9)$$

where ${}^oG_A^{Liq}$, ${}^oG_B^{Liq}$ and ${}^oG_{A_aB_b}^{Liq}$ stand for the Gibbs energies of the pure components and the associate in the system studied. ${}^EG_m$ is the excess Gibbs energy described by the Redlich-Kister polynomials [44] as the equation (7). y_A, y_B and $y_{A_aB_b}$ represent the mole fractions of the components and the associate in the liquid, which are expressed as:

$$y_A = n_{A_a} + a \cdot n_{A_aB_b} \quad (9a)$$

$$y_B = n_{B_n} + b \cdot n_{A_aB_b} \quad (9b)$$

$$y_{A_mB_n} = n_{A_mB_n} \quad (9c)$$

where n_{A_a}, n_{B_b} are the numbers of moles of A and B in equilibrium with $n_{A_aB_b}$ number of moles of the associate.

3.1.3 Binary oxide compounds

If the heat capacity data are available for the compounds, A_aB_b, in the A-B system, the general form of molar Gibbs energy functions for the compounds can be used as:

$${}^oG_{A_aB_b} - aH_A^{SER} - bH_B^{SER} - (a+b)H_O^{SER} = a + bT + cTlnT + dT^2 + eT^{-1} \quad (10)$$

where H_i^{SER} is the enthalpy of element at 298.15 K and 1 bar. The parameters *a*, *b*, *c*, *d* and *e* were optimized on the basis of the heat capacity data.

When the heat capacity data for the compounds are not sufficient enough to perform thermodynamic optimization, the empirical Neumann-Kopp rule (NKR) [45] is applied to predict the heat capacity of mixed oxides. After numerous application of the Neumann-Kopp rule, it is deemed to be able to give a reasonable estimation for most mixed oxides around room temperature. However, the accuracy of the prediction is substantially lowered at both low and high temperatures [46]. It cannot be regarded as a simple additive operation as the sum of the elements forming the compound. The rule was recently modified to increase the reliability of the estimation [47,48]. In a mathematical practice, when a ternary solid compound $A_aB_bC_c$ (C stands for the element O in the present thesis) is formed by a reaction of the binary compounds AC_1 and BC_2:

$$aAC_1\,(s) + bBC_2\,(s) = A_aB_bC_c\,(s) \quad (11)$$

it is assumed that:

$$C_p\,(A_aB_bC_c, s) = aC_p\,(AC_1, s) + bC_p\,(BC_2, s) \quad (12)$$

3.2 Case application of the models

In the present thesis, the substitutional solution model and associate solution model were applied to describe the liquid solution phase. Since no potential stoichiometric compounds or associates were reported for the BaO-CaO, BaO-SrO and BaO-MgO systems, the substitutional solution model was adopted. For the BaO-Al_2O_3 and BaO-SiO_2 systems, both models were employed and compared, in order to find out which can well reproduce the experimental and theoretical data. In the paragraphs below, the liquid phase in the BaO-MgO and BaO-SiO_2 systems were taken as examples to show the applicability of the two models.

3.2.1 Substitutional solution model

For the BaO-MgO binary system, there exist a molten phase, BaO-based and MgO-based solid solutions. Their molar Gibbs energy functions were described by the following expression:

$$G_m^{\varphi} - \sum H_i^{SER} = x_{BaO}\,{}^{o}G_{BaO}^{\varphi} + x_{MgO}\,{}^{o}G_{MgO}^{\varphi} + RT\left(x_{BaO}lnx_{BaO} + x_{MgO}lnx_{MgO}\right) + {}^{E}G_m \quad (13)$$

where x_{BaO} and x_{MgO} are the mole fractions of BaO and MgO. The excess Gibbs energy was described by the Redlich-Kister polynomials [44] as:

$${}^{E}G_m = x_{BaO}x_{MgO}\,{}^{l}L_{BaO,MgO} = x_{BaO}x_{MgO}[\,{}^{0}L + {}^{1}L(x_{BaO} - x_{MgO})] \quad (14)$$

where ${}^{l}L_{BaO,MgO}$ (l=0 and 1) is the interaction parameter between BaO and MgO to be optimized in the present thesis. According to the order of the interaction parameter in this term, the name of the term ${}^{l}L$ varies for different orders, for example, the regular solution model with the zeroth order (${}^{0}L$) and the sub-regular model with the first order (${}^{1}L$).. The general temperature dependent form, ${}^{l}L = a + bT$, was used. It should be stated that the terminal solid solutions (BaO-based and MgO-based solutions) were taken as pure oxides after literature evaluation.

3.2.2 Associate solution model

For the BaO-SiO_2 binary system, the molten phase is assumed to be constituted of three species (BaO, Ba_2SiO_4, SiO_2). The molar Gibbs energies were expressed as:

$$G_m^{Liq} - \Sigma H_i^{SER} = y_{BaO}\,{}^{o}G_{BaO}^{Liq} + y_{SiO_2}\,{}^{o}G_{SiO_2}^{Liq} + y_{Ba_2SiO_4}\,{}^{o}G_{Ba_2SiO_4}^{Liq} + RT\left(y_{BaO}lny_{BaO} + y_{SiO_2}lny_{SiO_2} + y_{Ba_2SiO_4}lny_{Ba_2SiO_4}\right) + {}^{E}G_m \quad (15)$$

where y represents the mole fractions of BaO, SiO_2 and the associate, Ba_2SiO_4, in the liquid. ${}^{o}G_{BaO}^{Liq}$, ${}^{o}G_{SiO_2}^{Liq}$ and ${}^{o}G_{Ba_2SiO_4}^{Liq}$ stand for the Gibbs energies of the

pure species in the liquid phase. Meanwhile, ${}^{E}G_m$ is the excess Gibbs energy described by the Redlich-Kister polynomials [44] as:

$$
\begin{aligned}
{}^{E}G_m = {} & y_{BaO} \cdot y_{Ba_2SiO_4}[\,{}^{0}L_{BaO,Ba_2SiO_4} + {}^{1}L_{BaO,Ba_2SiO_4}(x_{BaO} - x_{Ba_2SiO_4}) \\
& + {}^{2}L_{BaO,Ba_2SiO_4}(x_{BaO} - x_{Ba_2SiO_4})^2] + y_{SiO_2}y_{Ba_2SiO_4}[\,{}^{0}L_{SiO_2,Ba_2SiO_4} \\
& + {}^{1}L_{SiO_2,Ba_2SiO_4}(x_{SiO_2} - x_{Ba_2SiO_4}) + {}^{2}L_{SiO_2,Ba_2SiO_4}(x_{SiO_2} - x_{Ba_2SiO_4})^2 \\
& + {}^{3}L_{SiO_2,Ba_2SiO_4}(x_{SiO_2} - x_{Ba_2SiO_4})^3 + {}^{4}L_{SiO_2,Ba_2SiO_4}(x_{SiO_2} - x_{Ba_2SiO_4})^4]
\end{aligned}
\tag{16}
$$

where ${}^{l}L_{BaO,Ba_2SiO_4}$ and ${}^{l}L_{SiO_2,Ba_2SiO_4}$ (l=0,1,2 etc.) are the interaction parameters between different species to be optimized in the present thesis. The general temperature dependent form of the interaction parameter ${}^{l}L_{BaO,SiO_2} = c + d * T$ was used.

It should be mentioned that on the basis of the literature review in the introduction section, no data could be achieved on the mutual solubility between BaO and SiO_2 terminal phases.

3.3 Other models

A sub-lattice phase can be viewed as being composed of interlocking sublattices where the different components mix and occupy certain positions [26]. The solid phases may be characterized as ionic compounds if the metals form the cations and oxygen is the anion. A model was developed for the description of this kind of solids, named as compound energy model [49]. It can also be applied to describe the liquid phase. The compound energy model directly represents the Gibbs energy of the real or hypothetical compounds. In case of the deviation from the stoichiometric compounds, the neutral vacancy is introduced, the number of which is determined by the condition of electro-neutrality.

The ionic two sub-lattice model for describing the liquid phase was reported by Hillert et al. [16] within the frame of the compound energy formalism (CEF). The model is generally expressed as:

$$(C_i^{v_i})_P(A_j^{v_j}, Va^{-Q}, B_k^0)_Q \tag{17}$$

where each pair of parentheses denotes a sub-lattice where the cations (C), anions (A), vacancies (Va) and neutrals (B) are distributed. In order to maintain the electro-neutrality, the stoichiometric factors P and Q are calculated by the relations as:

$$P = \sum_i(-v_j)y_{A_j} + Qy_{Va} \tag{18}$$

$$Q = \sum_i(v_i)\, y_{C_i} \tag{19}$$

where y stands for the site fraction of the species.

The modified quasi-chemical model (MQM) was developed by Pelton et al. [18] to represent the thermodynamic properties of ionic liquids. The model

defines that the liquid phase has a strong tendency to order around specific compositions with certain physical or chemical phenomena [26]. The model has been used for various systems including oxide and silicate slags and salt systems.

3.4 Thermodynamic optimization

The thermodynamic optimization was performed using PARROT module in the Thermo-Calc software package [23]. It can fit the thermodynamic parameters to the experimental data available at stable or metastable state. The principle of data optimization is based on the least-squares method by fitting the calculated values on the basis of a model with observed quantities [50]. A collection of files is used during the assessment employing PARROT module, including SETUP file (models and thermodynamic parameters), POP file (experimental data for fitting), EXP file (experimental data to be plotted and compared) and MACRO files (quick calculation of various property diagrams). All the files can be prepared and edited in a text editor.

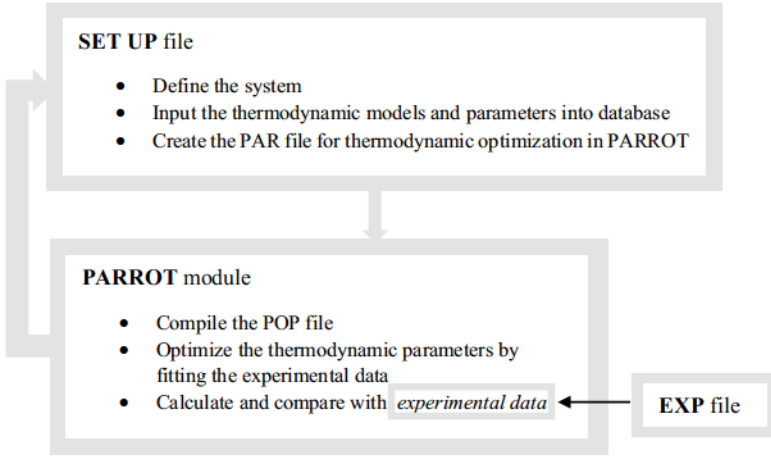

Figure 2. The flowchart of the optimization.

As can be seen in Figure 2, the basic thermodynamic optimization starts by running the SETUP file to define the system, input the thermodynamic models and parameters for various phases, and to create a workspace named as .PAR file. Then the collected experimental data will be stored in the .PAR file by compiling the POP file. At the beginning, the parameters are optimized one by one, by suspending other parameters and fitting to the selected group of the experimental data. During the optimization, due to the lack of experimental information, it may give too large or small variable, so the weight of each piece of experimental data has to be adjusted accordingly until a reasonable result is achieved. Intermittently, by using the MACRO file, the phase diagram or property diagram is calculated and compared with the experimental data, so that the validity and reliability of the thermodynamic parameters can be

evaluated. It is possible that the SETUP or POP file should be edited until reaching a satisfactory description of most experimental results. An overall optimization of all the variables and experiments is performed and some of the obtained parameters already obtained are slightly adjusted to achieve the 'best' fit.

Generally, it is difficult to draw the conclusion whether the final optimized results are in a good quality or not, since it mostly depends on the availability of experimental data and a good understanding of thermodynamics and modelling. One possible way to define the quality of the optimized thermodynamic parameters is whether it can well reproduce most of the experiments and facilitate to extrapolate into higher order systems. Consequently, personal judgment and experience play an indispensable role in optimization process.

4. Experimental

Although it is widely accepted that calculation with assistance of computers is more economical and less time-consuming than experimental investigation, the realization of most thermodynamic assessment and optimization starts with reliable experimental measurements [51]. Experimental determination of phase diagram is realized by observing phase existence, phase coexistence and transitions using various analysis methods. Application of multiple experimental techniques is beneficial for studying ceramic or slag oxide system, exhibiting a broad range of physical behaviour. The choice of techniques is tailored by considering the fact that one technique for one region of the phase diagram studied may not be suitable for another area. Assembling the data of phase relationships serves as the foundation to construct a phase diagram. The interpretation of the data is within the scope of Gibbs phase rule, crystal chemistry and the limitations of the experimental techniques employed [51].

The experimental techniques for characterizing the phase equilibrium are generally classified into two groups: static and dynamic. Static methods are based on the determination of phase existence or coexistence after equilibrating a sample under constant temperature and pressure in a reasonable lengthy of time. The quenching technique is commonly performed by rapid cooling an equilibrated sample to room temperature. It allows room temperature analysis to attain high temperature phase equilibrium data of the quenched sample. Dynamic techniques are based on the measurement of property change when the system is undergoing phase transition. Differential thermal analysis (DTA), differential scanning calorimetry (DSC) and thermal gravity analysis (TGA) are mostly applied as the assistance of dynamic techniques.

For systems with sluggish kinetics, sufficient diffusion time is required, so the static methods are preferred. The high temperature quenching experiments conducted in the present work were based on static method. Therefore, the following paragraphs are all on the basis of this approach.

4.1 Experimental difficulties associated with BaO

Critical literature survey was made concerning the choice of the starting material as the source of BaO since it is the basis of all the oxide systems studied in the thesis. According to the literature, the major experimental difficulties working with BaO are (i) reactivity with the containment vessels by forming certain compounds at elevated temperatures; (ii) reactivity with the moisture

and carbon dioxide in the atmosphere; (iii) the presence of a low temperature eutectic reaction in the BaO-$BaCO_3$ system [52-54]; and (iv) high vapour pressure of BaO in high-baria compositions above 1673 K.

Levin and McMurdie [55] and Baker [54] both observed the reaction of free BaO with platinum containers. In the study of BaO-Pt system in air, Schneider and McDaniel [56] reported the phase diagram of the BaO-Pt system that a compound forms and stabilizes between 1473 K and 1523 K. The finding was confirmed by Gallagher et al. [57] by successfully synthesizing the compound. In the personal experimental work at the beginning stage of the whole study, the author observed that BaO 'attacks' the platinum foil by dissolving platinum and forming yellowish powders when platinum foil was used as the substrate for holding the BaO-containing samples. Therefore, in the present experimental work, the platinum foil was avoided in order not to contaminate the studied systems. The equilibration temperatures for the phase equilibria study throughout the experimental work are all above 1350 K, so the occurrence of the eutectic reaction between BaO and $BaCO_3$ can be avoided.

4.2 Materials and sample preparation

Based on the discussion above and literature survey, $BaCO_3$ is accepted as the raw material to acquire BaO. Commercial powders of $BaCO_3$, MgO, Al_2O_3 and SiO_2 were used as starting materials for sample preparation. As mentioned in the previous chapter, the use of platinum foil was avoided in order not to contaminate the systems studied. Different commercial crucibles were employed as the substrates for holding the samples, depending on the targeted systems. All details about the powders and the crucibles are summarized in Table 1.

Table 1. Details of the powders and crucible used in sample preparation.

Chemicals	Purity, wt%	Supplier
$BaCO_3$	99.95	Alfa Aesar
MgO	99	Sigma-Aldrich
Al_2O_3	99.99	Sigma-Aldrich
SiO_2	99.99	Umicore
MgO substrate	99	Self-made by pressing, sintering and drilling
Al_2O_3 crucible	>99.5	FRIATEC
SiO_2 crucible	>99.98	OM Lasilaite Oy

The powders were dried at 423 K for 24 h to remove the moisture. Then they were mixed with specific molar ratio and ground in an agate mortar, and finally pelletized to the diameter of 5 mm and thickness of 4 mm with a pressing tool. The mass of each sample was less than 0.2 g by considering the fact that small bulk of the samples facilitates a good quenching. These samples were used to measure the liquidus of each system. The samples employed to study the phase stabilities and relations of the stoichiometric compounds were pressed into the diameter of 9 mm and height of 10 mm. The mass of each sample was around 2 g.

For the $BaO-Al_2O_3$ and $BaO-SiO_2$ systems, the commercial crucibles made of Al_2O_3 and SiO_2 were used separately, since Al_2O_3/SiO_2 is the component of the $BaO-Al_2O_3/SiO_2$ system studied, in this way, the purity of the systems studied was preserved. For the BaO-MgO system, the substrate was prepared from the pure MgO powder, which was pelletized, sintered and drilled to cylinder shape (D=18 mm and h=4 mm) with an inner diameter of 10 mm and depth of 2 mm. The arrangement of the substrate with the sample is graphically presented in the next section.

4.3 Experimental apparatus

The experimental work was divided into two batches where one batch aimed at investigating the liquidus of the systems, and another one focused on solid state phase equilibria of the stoichiometric compounds in the systems. Therefore, two types of furnaces were employed and are separately introduced in the following paragraphs.

For the first batch, considering the requirements of fast quenching and requirement of high temperature (above 1723 K), the equilibration was accomplished in the furnace with a vertical Al_2O_3 work tube inside, as illustrated in Figure 2. The hot zone of the furnace was preliminarily determined by establishing and comparing the thermal profiles at 1173 K, 1473 K and 1773 K. The furnace was found to have 6 cm long hot zone that allowed flexibility in positioning the sample and sample holder. A calibrated S-type thermocouple was connected to a Keithley 2010 multi-meter, and a cold junction compensation was connected to a Keithley 2000 multi-meter to measure the ambient room temperature with a Pt100 sensor. The data of temperature throughout the experiments were collected using a NI LabVIEW temperature logging program. The overall accuracy of the measurements was estimated as ±2 K. The top and bottom of the work tube were open to the atmosphere. The rolled copper tubes, with water running inside, were employed for cooling the furnace.

As it can be seen from Figure 3, the pelletized sample was placed in the MgO (or Al_2O_3 or SiO_2) substrate and suspended, using a platinum wire, from the bottom of the tube and raised into the hot zone. The position of the sample and substrate is shown in detail in Figure 4.

For another batch of the experiment to determine the phase relations of the stoichiometric compounds, a horizontal tube furnace (Figure 5) was employed for the equilibration experiments. The same method as introduced above was used to find the hot zone of this furnace. The details of the method can also be found in the publications [II,III]. The samples prepared in this batch contained over 60 % BaO, and by taking into account the hydration of high-baria compositions and the formation of barium peroxide (BaO_2) at low temperatures, the experiment was conducted under the protection of gas mixture of argon (99%) and hydrogen (1%) and a filter was connected to remove moisture in the gas before flushing the gas into the furnace. The samples with varying compositions of BaO and Al_2O_3 were placed in the alumina crucible boat. For

the $BaO\text{-}SiO_2$ system without Al_2O_3, a net made of platinum wire was placed under the samples to avoid the contact with alumina crucible boat. The temperature in this study was low (below 1573 K) and the phenomenon that BaO attacks Pt was not observed.

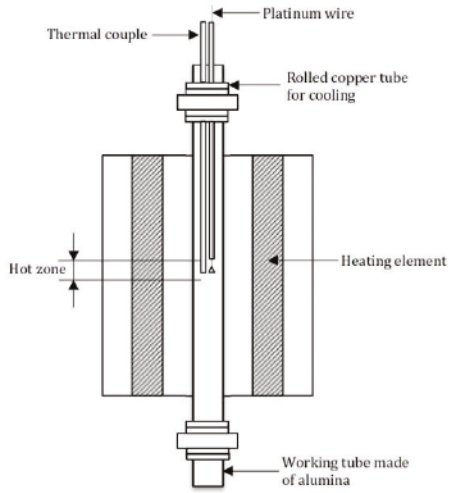

Figure 3. Schematic picture of the vertical tube furnace.

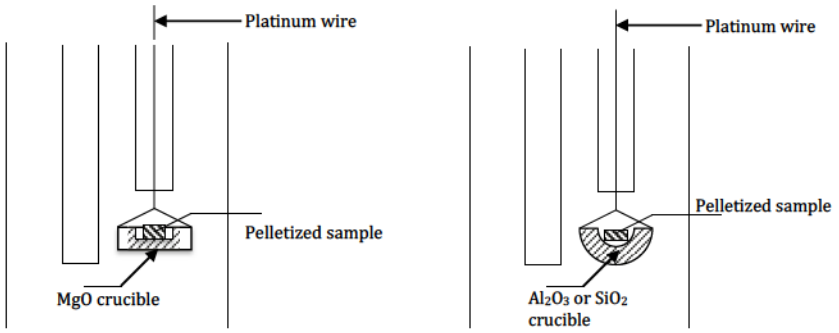

Figure 4. Arrangement of the sample and sample holder.

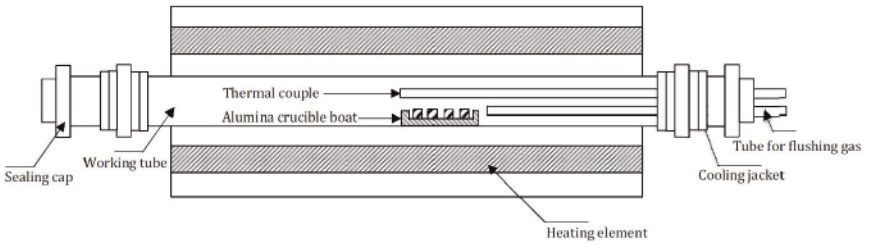

Figure 5. Schematic picture of the horizontal furnace and arrangement of the samples.

4.4 Equilibration time

Careful consideration was given to the equilibration time. Prior to the experiments, a few trials were conducted to verify the suitable equilibration time.

For the experiments aiming at measuring the liquidus of the system, time series of 4 h, 8 h, 12 h and 24 h was performed as the pre-experiments. It was found that the equilibrium was achieved within 8 h at and above 1673 K, and longer diffusion time, 24 h, was needed at 1623 K. The attainment of the equilibrium state was confirmed by two means, (i) for the quenched samples at various hours, checking the phases via backscattered electron (BSE) graphs whether co-existence of molten phase and crystals (or solid-solid phases) at the given temperatures can be observed, and (ii) the chemical analysis employing Scanning Electron Microscopy/Energy Dispersive X-ray Spectroscopy (SEM/EDS) to check the homogeneity of the phases at different locations of the samples whether they are consistent.

For the experiments investigating the phase relations of stoichiometric compounds in the systems, considering the mass of the each sample (≈2 g), longer equilibration time of 14 h, 20 h, 48 h and 96 h was tested. It was concluded that the equilibration time ranged from 20 h to 48 h, depending on the systems under investigation. The more detailed information can be obtained from the publications in this thesis.

4.5 Experimental procedure

For the experiment using vertical tube furnace (Figure 2), the pelletized sample was placed in the crucible, suspended and elevated using a platinum wire from the bottom of the work tube to the hot zone. The top and bottom of the work tube were open to the atmosphere. Then the sample was held at target temperature and time to complete the equilibration. After the equilibrium was reached, a bottle of mixture of ice and water was placed under the bottom of work tube. The quenching happened that the sample and sample holder were rapidly released by pulling the platinum wire. The quenched sample was dried and mounted in epoxy resin. In order to acquire the cross section of the mounted sample, the solidified epoxy resin was ground and polished without introducing water and lubricant. The polished sample was carbon coated, after which it was ready to be analysed. This batch of experiments focused on the temperature varying from 1623 K to 1923 K.

For another batch of experiments investigating phase relations of stoichiometric compounds, the crucible boat with samples inside was placed at the hot zone of the furnace with flowing gas of Ar (99%) and H_2 (1%). Before the equilibration experiment, the furnace was flushed with gas mixture for half an hour to remove the extra air in it. The quenching was conducted by using a hook to pull the boat out of the furnace and placing into the icy water. In order to avoid water and possible contaminations to the samples, they were left on the crucible boat when quenching occurred. This batch of experiments was made from 1423 K to 1523 K.

4.6 Experimental analysis

For the experiments studying the liquidus of the oxide systems, the carbon coated samples were analysed with SEM/EDS to identify and quantify various phases studied. The microscope can provide images of the sample by scanning with a focused beam of accelerated electrons. The accelerating voltage was 15 kV. The EDS detects x-ray emitted from the sample bombarded by the beam to characterize the elements of the analysed area. The standards were Barite for Ba, Apatite for Ca, Olivine for Mg, Albite for Al, and Quartz for Si. To acquire more accurate chemical analysis, Electron Probe X-ray Micro-Analyser (EPMA) with five wavelength dispersive spectrometers at Geological Survey of Finland (GTK) was employed. It is a non-destructive method for elemental analysis at the surface of the sample with the sensitivity at the level of ppm. The analysis were performed on every sample at different locations of the phases with total 10 points. The accelerating voltage was 15 kV and beam current was 6 nA. The analysed lines and standards used for each element were O Ka (hematite), Ba La (barite), Al Ka (alumina) and Si Ka (quartz).

Since the mass of the samples achieved from the experimental investigation of phase relationships of the compounds in the oxide systems was large enough, each sample was divided into two parts that one portion was analysed by SEM/EDS and X-ray powder diffractometer with CuKα radiation were applied to analyse the other portion.

5. Results and discussion

The CALPHAD technique is unable to predict the existence of the phase unless it is experimentally confirmed and included into the thermodynamic assessment. Therefore, it should be noted that even if thermodynamic modelling is convenient and efficient, experimental work is required as the foundation to realize the completion of thermodynamic modelling with a high reliability. The present thesis focuses on (i) the experimental investigation of the phase equilibria of various oxide systems in the regions where data are scarcely available, (ii) thermodynamic assessment and optimization to acquire sets of thermodynamic parameters to well describe the oxide systems, and (iii) test the feasibility and validity of various thermodynamic models applied to describe the behaviour of the molten phase in the systems. Consequently, the measured phase equilibria data, optimized thermodynamic parameters and calculated phase diagrams and property diagrams of various oxide systems are presented as the results. For each system included in the present thesis, experimental work started by investigating the phase equilibria at elevated temperatures (above 1300 K) in the regions where the availability of data was poor. On the basis of the personal experiments and literature data, the thermodynamic modelling was performed using various models. The optimization work was conducted using PARROT module in the Thermo-Calc package [23], until a set of self-consistent thermodynamic parameters was obtained that the experimental data can be reproduced. In total, six binary systems were experimentally and thermodynamically studied. The detailed descriptions of the experimental and thermodynamic modelling results are presented in the Appendices [I-V], but a summary with a discussion is given below.

5.1 Evaluation of the thermodynamic data of BaO

As the whole present work is concentrated on BaO-containing oxide systems (BaO-SrO-MgO-CaO-Al_2O_3-SiO_2), the accuracy and reliability of the thermodynamic data of BaO is the key to make the thermodynamic assessment reliable. Therefore, the evaluation of the thermodynamic properties and parameters to describe the BaO is necessary. This evaluation work was conducted and presented in a technical report [58] where the detailed introduction and discussion are provided. The melting point, heat capacity, enthalpy increment, enthalpy of formation and entropy of formation of the BaO

was assessed and compared in the report. Three primary results shown in the Figures 6, 7 and 8 illustrate that the thermodynamic parameters were consistent with the SGTE substance database 1994 [37], and thus were employed to describe the BaO in the entire work. The thermodynamic parameters of BaO in the database [37] are presented as the Gibbs energy functions with temperature intervals, which can be found in the publications [I, II, IV, V].

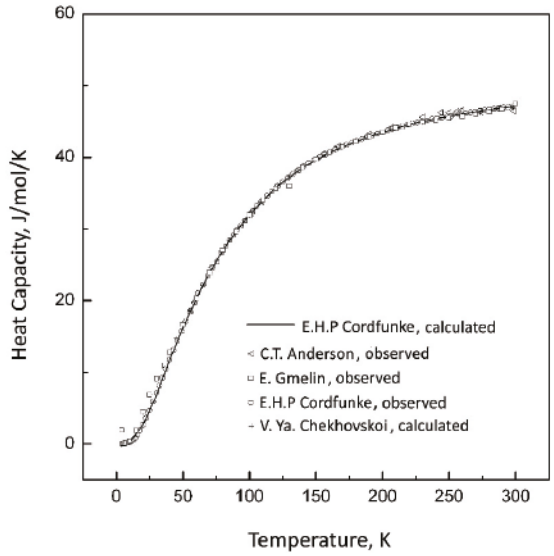

Figure 6. A comparison of the heat capacity data of BaO below 300 K [58].

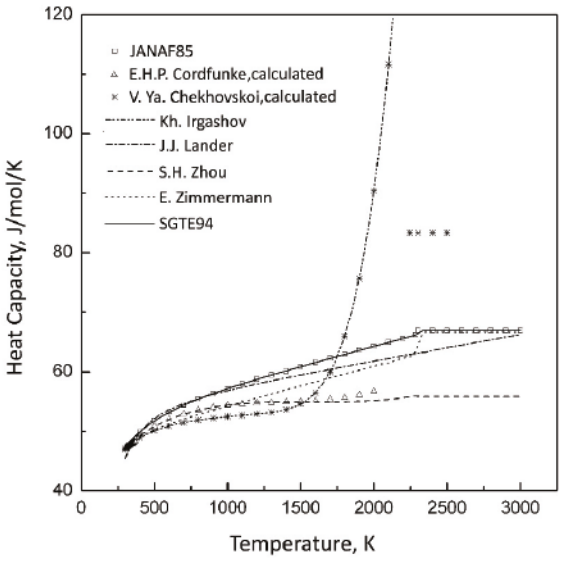

Figure 7. A comparison of the heat capacity data of BaO above 300 K [58].

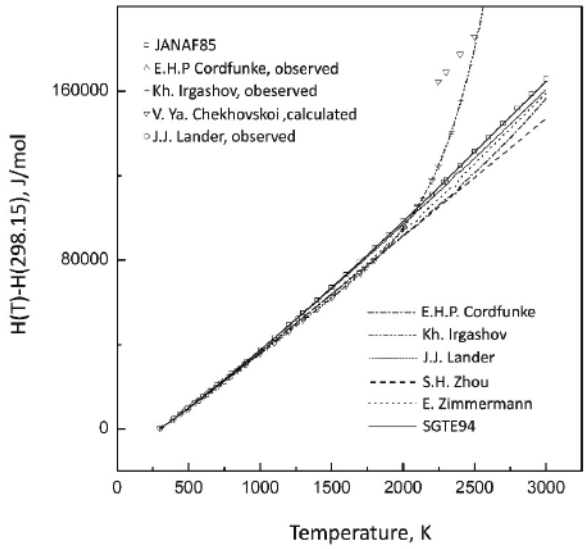

Figure 8. A comparison of enthalpy increment of BaO [58].

5.2 The BaO-MgO system

Due to the high melting points of BaO and MgO, 2196 K and 3215 K respectively, the experiments are hard to conduct, and hence the phase equilibrium data is poorly known. Regarding the liquidus and eutectic reaction, a large discrepancy can be found between the measurements by Wartenberg and Prophet [59] and the calculations by Van-der Kemp et al. [60] and Shukla [61]. Based on the high temperature equilibration and quenching experiments in publication [I], no molten phase could be observed below 1873 K and the no solubility was found between BaO and MgO. The results of the calculated work in publication [I] are compared with the literature data and shown in Figure 9. By using only four data points, Wartenberg [59] constructed the phase diagram of the BaO-MgO system, and the melting point of MgO in his work is largely different from those reported by Mcnally et al. [62], Schneider [63] and Ronchi and Sheindlin [64]. So the phase diagram constructed by Wartenberg [59] is inconvincible compared with the general accepted approaches to determine the phase diagram [51]. Considering the fact that no information can be found above 1900 K as a result of the high experimental temperature, the calculated phase diagram in the publication [I] accords with the modelling work by Shukla [61]. More experimental measurements are necessary in order to describe the liquid behaviour above 2000 K.

5.3 The BaO-CaO system

The only previous experimental measurement of the BaO-CaO system was conducted by Flidlider et al. [65], indicating a very low mutual solubility of barium and calcium oxides in the solid state, by using the calorimetric method.

However, the specific values of the solubility between the two components were absent from their work. Due to the absence of experimental data, the thermodynamic modelling was conducted in publication [V] by considering the calculations by Van-der Kemp [60], Shukla [61] and Seo et al. [66]. The calculated phase diagram is shown in Figure 10. The calculated solubility ranges agree well with the work by Van-der Kemp [60] and Shukla [61]. The same recommendation as for the BaO-MgO system is made that liquidus data at temperatures above 2000 K is needed.

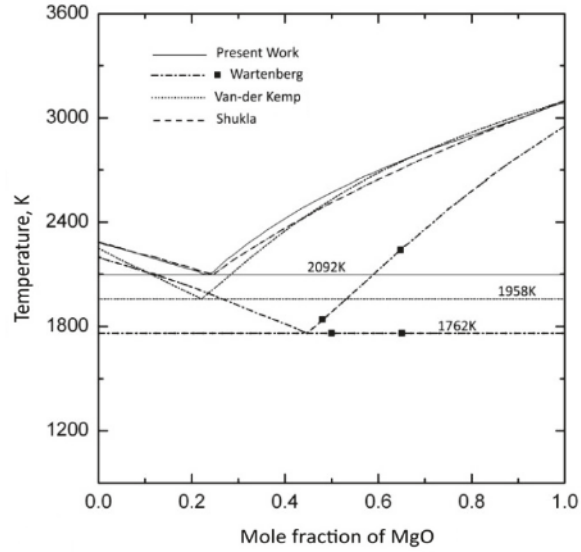

Figure 9. Calculated phase diagram of the BaO-MgO system compared with literature data [I].

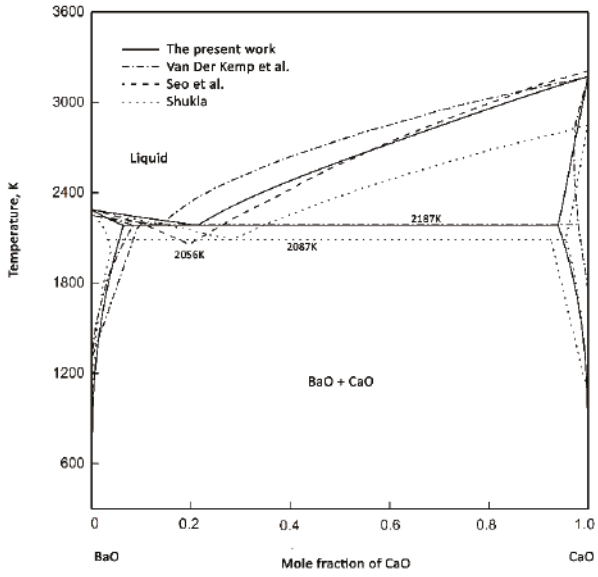

Figure 10. Calculated phase diagram of the BaO-CaO system compared with literature data [V].

5.4 The BaO-SrO system

By means of mass spectrometry, Van Der Kemp and Oonk [67] determined the excess molar Gibbs energy for barium and strontium oxides in the temperature range 1430 K to 1530 K. Based on these results, the phase diagram of BaO-SrO was calculated and the consolute temperature for solid demixing was reported to be T=1334 K. The solid state miscibility gap was delineated by Jacob and Varghese [68] on the basis of the X-ray diffraction study. In publication [V], the thermodynamic assessment was executed by considering these two sets of data. The calculated phase diagram with the literature data is presented in Figure 11. It can be seen that the calculated solid state immiscibility agrees well with the measurement by Jacob and Varghese [68]. Since Van Der Kemp and Oonk [67] used regular solution model with symmetric excess Gibbs energy, the peak of the immiscibility of the two solids was calculated to be 0.5 mol% SrO and 1334K.

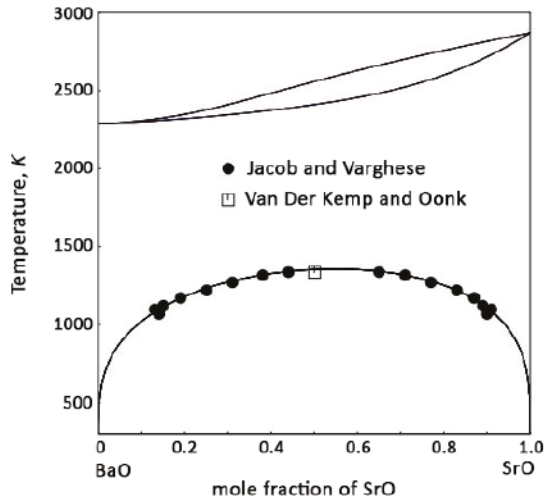

Figure 11. Calculated phase diagram of the BaO-SrO system compared with literature data [V].

5.5 The BaO-Al_2O_3 system

Literature data on experimental and thermodynamic modelling are available to describe the BaO-Al_2O_3 system in most regions, as can be found in the publication [II]. The major disagreement lies in the phase relations in the high-baria corner. The B_3A ($Ba_3Al_2O_6$), B_4A ($Ba_4Al_2O_7$), B_5A ($Ba_5Al_2O_8$), B_7A ($Ba_7Al_2O_{10}$), B_8A ($Ba_8Al_2O_{11}$) and $B_{10}A$ ($Ba_{10}Al_2O_{13}$) were reported by Appendino [69] (experimental) and Shukla [61] (calculated) to be stable phases above 1200K. However, in the works by Purt [70], Toropov and Galakhov [71] and Kovba et al. [72] based on XRD analysis, only B_3A, B_4A and B_7A were confirmed to be stable above 1200 K. These findings were consistent with the phase relations determined in the present work, as shown in the publication [II]. The liquidus of the phase BA were studied using high temperature equilibration quenching technique and analysed with SEM/EDS and EPMA, and the

measured phase equilibria can be achieved in the publication [II]. The representative microstructure of the quenched samples denoting the equilibrium between molten phase and BA is presented in Figure 12. Clear scratches can be observed due to the dry polishing method employed to avoid the corruption of the samples contacting with polishing liquid.

The substitutional solution model and associate solution model (introduced in Chapter 3) were applied to describe the molten phase in the BaO-Al_2O_3 system. As can be found in the technical report [58] that the melting behaviour of the liquid was thermodynamically modelled, but the liquid in equilibrium with BA phase was poorly described.

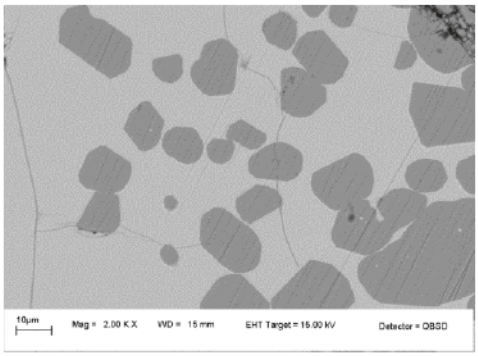

Figure 12. Backscattered scanning electron micrographs of the quenched BaO-Al_2O_3 sample at 1723 K. The crystals are BA phase and non-crystalline continuous phase is molten phase [II].

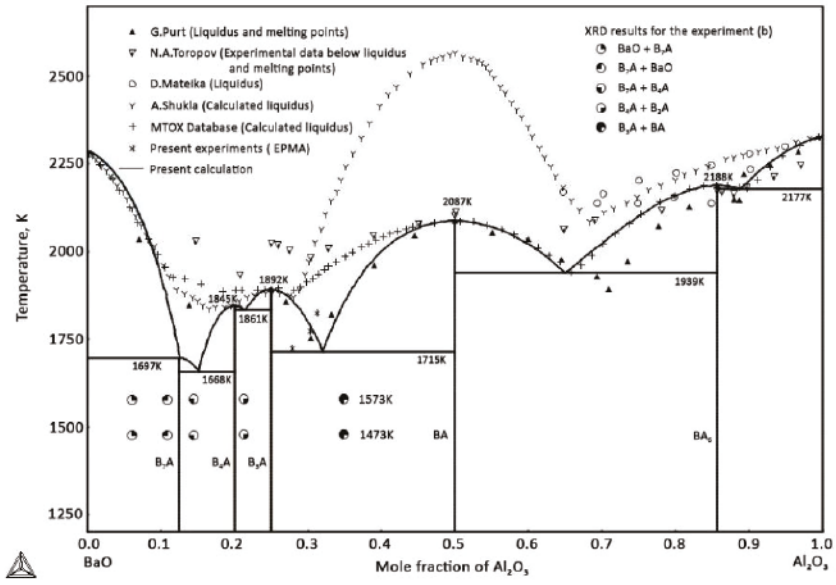

Figure 13. Calculated phase diagram of the BaO-Al_2O_3 system compared with literature data [II].

With the newly added experiments reported by the publication [II] and the calculated liquidus from MTOX oxide database [24], the thermodynamic re-assessment using associate solution model was performed and the

thermodynamic description of this system was improved. The liquidus across the whole compositional range and the calculated melting points of B_3A, B_4A, BA and BA_6 are well fitted with the experimental determinations, as shown in the calculated phase diagram in Figure 13. An agreement was achieved regarding the calculated thermodynamic properties compared with literature data, including heat capacities of BA, B_3A, BA_6, B_4A and B_7A, enthalpy of mixing for liquid, and heat contents (H_T-H_{298}) of BA. The comparison of the calculated properties and literature data can be found in the publication [II], and a set of consistent thermodynamic parameters is presented in the publication [II]. In order to further improve the description of this binary system across the whole compositional range, (i) the experimental melting behaviour of the B_7A is needed but it is extremely challenging that the experiment involves high-baria samples at temperature above 1800 K, and (ii) the associate model with two associates, B_3A and BA, is recommended for a trial to describe the liquid curve between the two phases.

5.6 The BaO-SiO_2 system

The phase diagram and thermodynamic properties of the BaO-SiO_2 system were extensively investigated by means of experimental determination and thermodynamic modelling. The critical literature review can be obtained in the publications [III, IV]. According to the experimental results made by the author [III,IV] and from literature data [73-76], seven stoichiometric compounds were experimentally confirmed. They are Ba_3SiO_5 (B_3S), Ba_2SiO_4 (B_2S), $BaSiO_3$ (BS), $Ba_2Si_3O_8$ (B_2S_3), $Ba_3Si_5O_{13}$ (B_3S_5) and $Ba_5Si_8O_{21}$ (B_5S_8). The phase relations of the stoichiometric compounds in the high BaO side were identified presented in the publication [III,IV]. In the SiO_2-rich corner, a discrepancy exists that a reverse S-shaped liquid curve was experimentally detected by the author [III], Greig [77] and Ol'Shanskij [78], while a liquid miscibility gap was calculated by Shukla [61]. No liquid immiscibility was observed based on the experimental results achieved by the author [III]. The experimental determinations [III] by EPMA and EDS are listed in Table 2. The melting behaviour of the B_3S was difficult to investigate due to the restriction of the furnace with the maximum temperature of 1973 K. Therefore, the thermodynamic assessment of the BaO-SiO_2 system was based on the available experimental data measured by the author and from the selected literature.

Substitutional solution model and associate solution model were employed to describe the liquid phase. For the associate model, one associate (Ba_2SiO_4) and two associates ($BaSiO_3$ and Ba_2SiO_4) were applied to test which can better depict the melting behaviour of the molten phase. In the publications [IV] and [V], three sets of optimized thermodynamic parameters can be found that can reproduce the experimental data to different extents. The calculated phase diagrams using assessed thermodynamic parameters are shown in Figures 14, 15 and 16. After comparison, the description of the behaviour of the molten phase across the whole compositions was largely improved by using associate solution model. At the same time, with two associates in the associate solution

model, the liquidus between B_2S and BS presents a slight improvement than using the associate solution model with one associate.

Table 2. Comparison of the phase composition of molten phase and crystals analysed by EPMA and EDS [III].

Temperature (K)	Phase	EPMA (mol %)		EDS (mol %)	
		SiO_2	BaO	SiO_2	BaO
1913	Molten phase	86.55	13.44	87.7	12.3
	SiO_2	99.95	0.05	99.8	0.2
1893	Molten phase	86.99	13.01	87.5	12.5
	SiO_2	99.93	0.07	99.9	0.1
1873	Molten phase	79.65	20.35	81.6	18.4
	SiO_2	99.96	0.04	99.8	0.2
1823	Molten phase	77.40	22.60	78.2	21.8
	SiO_2	99.93	0.07	99.8	0.2
1773	Molten phase	76.60	23.40	77.6	22.4
	SiO_2	99.92	0.08	99.8	0.2
1723	Molten phase	74.35	25.65	75.7	24.3
	SiO_2	99.92	0.08	99.9	0.1
1703	Molten phase	74.53	25.47	75.1	24.9
	SiO_2	99.90	0.10	99.8	0.2
1673	Molten phase	73.57	26.43	73.9	26.1
	SiO_2	99.90	0.10	99.8	0.2
1623	BS_2	67.36	32.64	66.5	33.5
	BS	51.71	48.29	51.5	48.5
	SiO_2	99.92	0.08	99.0	1

The illustrations of how the associates behave in the liquid phase are indicated in Figures 17, so that one can understand how the associate model works. However, the associate model should be regarded as a mathematical approach for the expression of the Gibbs energy functions since the existence of associates in the oxide systems studied in this thesis was insufficiently determined.

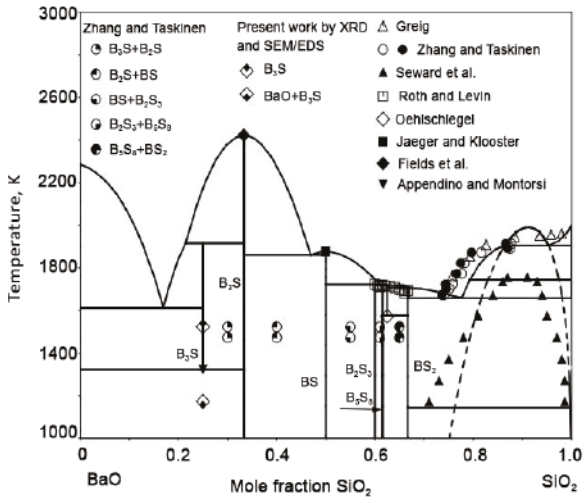

Figure 14. Calculated phase diagram of the BaO-SiO_2 system using substitutional solution model for the description of molten phase, compared with literature data [IV].

The thermodynamic properties, for example, heat capacities of B_3S, B_2S, BS, B_2S_3, B_3S_5 and B_5S_8, enthalpy increments (H_T-H_{273}) of the liquids with the composition of BS_3, activities of BaO and SiO_2 in glasses and melts and Gibbs energy of mixing at 1970 K, were calculated based on the thermodynamic

parameters acquired. The details can be extracted from the publications [IV] and [V]. The further work should be concentrated on the construction of the liquidus in the high-baria corner although it is demanding that the BaO tends to vaporize in this region at temperatures above 1673 K.

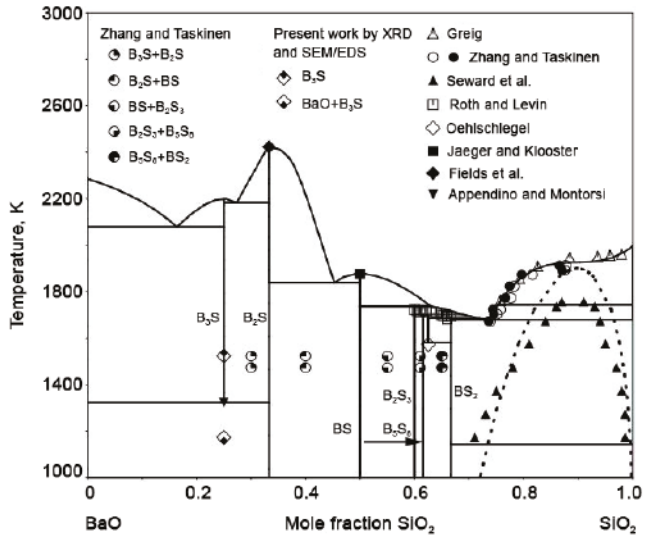

Figure 15. Calculated phase diagram of the BaO-SiO_2 system using associate solution model with B_2S as an associate for the description of molten phase, compared with literature data [IV].

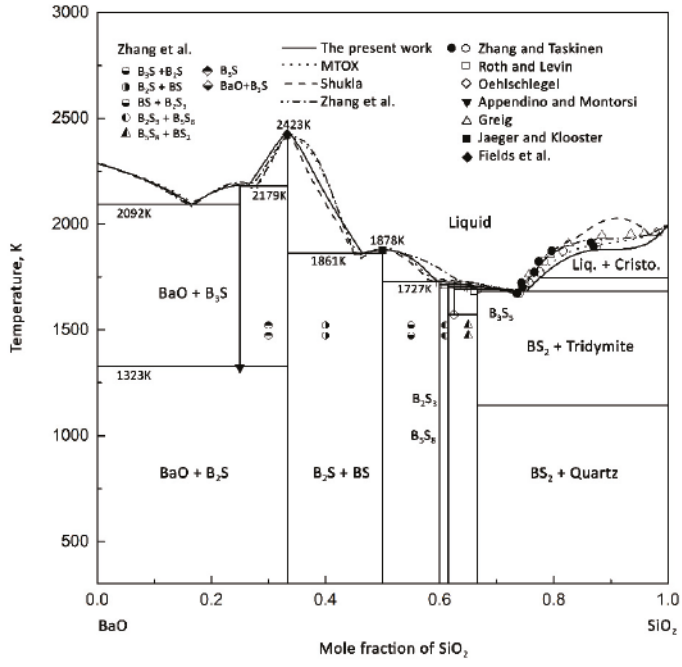

Figure 16. Calculated phase diagram of the BaO-SiO_2 system using associate solution model with B_2S and BS as associates for the description of molten phase, compared with literature data [V].

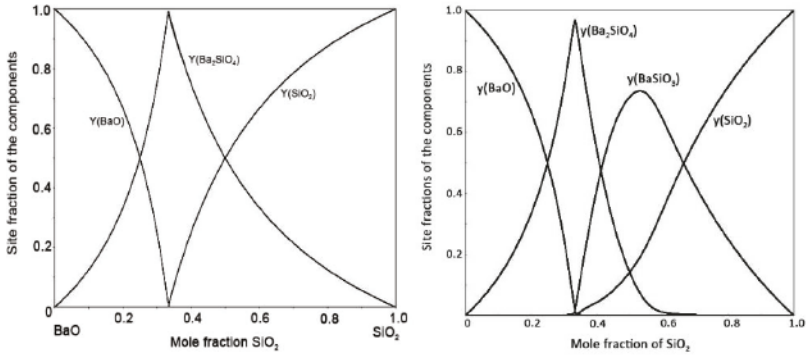

Figure 17. Calculated site fractions of various species in the liquid phase. On the left, one associate was employed in the associate solution model. On the right, two associates were used [IV,V].

5.7 The SrO-SiO_2 system

Strontium resides in the same group as barium in the periodic table, so they may exhibit similar interactions with silicon oxide, for example, formation of the stoichiometric compounds (B_2S and S_2S, BS and SS, B_3S and S_3S) with high melting points. The major difference is the shape of the liquidus in the SiO_2-rich corner. By means of quenching method combined with microscopic examination, Kracek [79] constructed the cristobalite liquidus in the alkali oxide-silica system (Mg, Ca, Sr, Ba, Li, Na, K, Rb and Cs). A reverse S-shaped liquid curve from BaO to Cs_2O was indicated and the existence of a miscibility gap was reported for the MgO to SrO systems. This reverse S type cristobalite melting curve was also confirmed by Ol'Shanskij [78].

The same amount attention as the BaO-SiO_2 system has been paid to the SrO-SiO_2 system due to its wide application in glass and ceramic technology. A collection of phase equilibria data, thermodynamic properties and thermodynamic modelling can be obtained by literature survey. After critical literature evaluation, the thermodynamic modelling was performed by the author using associate model to describe the molten phase. The calculated diagrams according to the optimized thermodynamic parameters by the author allow a good fit with the literature data, as can be found in the publication [V]. The calculated phase diagram compared with the experimental and modelling data is presented in Figure 18. A good agreement was achieved although the calculated temperature of the eutectic reaction, Liquid → SS + Tridymite, is slightly higher than the measured one. The calculated results concerning the thermodynamic properties, for example, activities of SrO and SiO_2 in the melt, enthalpy increments (H_T-H_{273}) with the composition of SrO·2SiO_2, enthalpy increments (H_T-H_{298}) of the S_2S and SS phases, are all included in the publication [V]. Future study should concentrate on the phase relationships of the S_3S, S_2S and SS phase above 1200 K, the decomposition temperature of S_3S and liquid immiscibility in the SiO_2-rich region above 2000 K.

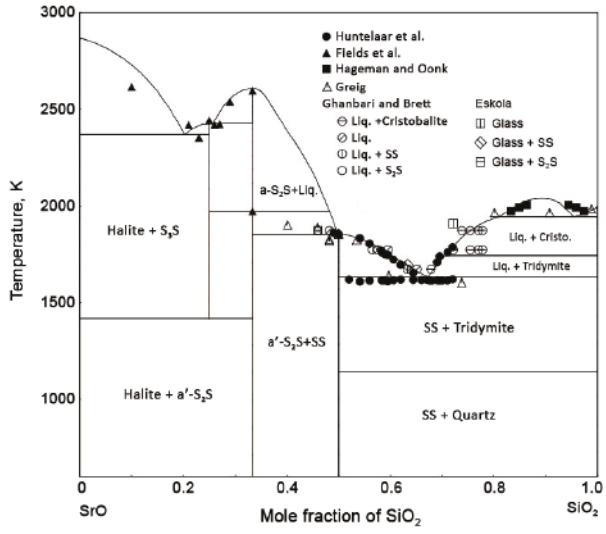

Figure 18. Calculated phase diagram of the SrO-SiO_2 system using associate solution model with S_2S as an associate for the description of molten phase, compared with literature data [V].

5.8 The BaO-SiO_2-Al_2O_3 system

When it comes to ternary oxides system, due to the complexity of the phase equilibria, such as, the formation of ternary compounds and solid solutions [80], only few experimental data are available in the literature, especially at the temperatures above 1673 K. New experimental data is beneficial for thermodynamic optimization of the ternary system and contributes to update the knowledge of the glass ceramics prepared based on celsian ($BaO{\cdot}Al_2O_3{\cdot}2SiO_2$).

As can be found in the work by Zhang and Taskinen [81], based on the XRD results, the authors successfully prepared celsian phase by solid state mixing, 96 h equilibration at 1473 K, as can be found in Figure 19. The molten phase in equilibrium with the celsian phase ($BaO{\cdot}Al_2O_3{\cdot}2SiO_2$) were experimentally investigated by SEM/EDS and XRD. By using MTDATA software [25], the isothermal sections at 1673 K, 1773 K, 1873 K and 1973 K were calculated. Experimental information regarding the isothermal sections at elevated temperatures are necessary in order to perform thermodynamic assessment and establish the thermodynamic database of the BaO-SiO_2-Al_2O_3 system. Future thermodynamic optimization of the ternary system will take into account the present measurements, assessed binary systems and updated data.

6. Conclusions

By means of the experimental equilibration-quenching and CALPHAD techniques, the phase diagrams and thermodynamic property diagrams of the BaO-CaO, BaO-MgO, BaO-SrO, BaO-Al_2O_3, BaO-SiO_2 and SrO-SiO_2 systems were produced. The sets of self-consistent thermodynamic parameters optimized in the present work contribute to the extrapolation into higher order oxide systems and the establishment of the thermodynamic database for future industrial application.

6.1 Experimental

Phase equilibria were experimentally investigated in the systems of BaO-CaO, BaO-MgO, BaO-Al_2O_3 and BaO-SiO_2. Two types of experimental set-ups were utilized for different purposes. For the construction of the liquidus at temperatures between 1623 K and 1973 K in the selected systems, the vertical furnace (Figure 2) was used to facilitate a fast quenching. Horizontal furnace (Figure 4) flushed with protective gas was applied to study the phase relations in the high-baria region. The experimental data acquired in the present thesis clarified the systems where less information is available and disagreements exist. The solid state phase equilibria were observed for the BaO-MgO system which corresponds with the modelling results. In the BaO-Al_2O_3 system, the liquidus in equilibrium with the $BaAl_2O_4$ phase was measured, and the phase relations at 1473 K and 1573 K were detected in the BaO-rich corner. The new data contribute to depict the complicated phase relationships of the stoichiometric compounds and to provide updated information for thermodynamic modelling work. A stable miscibility gap can be observed in the SiO_2-rich region in most of the silicate systems. However, in the present work, based on the phase equilibria determination, a reverse S shape liquidus was constructed in the SiO_2-rich region, which strengthens the support for a collection of work reporting the liquid curve of this shape instead of a stable miscibility gap by some other studies. The phase relations in the BaO-rich region and the phase stability of the Ba_3SiO_5 were determined and taken into account for thermodynamic assessment of this system.

6.2 Thermodynamic modelling

By means of the CALPHAD technique, the phase diagram and thermodynamic data in the BaO-CaO, BaO-MgO, BaO-SrO, BaO-Al_2O_3, BaO-SiO_2 and SrO-SiO_2 systems were critically evaluated. On the basis of the evaluated literature data and the experimental data acquired in the present thesis, thermodynamic assessments were performed using the PARROT module in the Thermo-Calc software package [23]. The Gibbs energy functions in terms of temperature and composition describing each phase in various systems are presented. For the thermodynamic modelling of the BaO-Al_2O_3 and BaO-SiO_2 systems, both substitutional solution model and associate solution model were employed to describe the liquid phase. By comparing the calculated phase diagrams and thermodynamic properties adopting two kinds of models, no difference was found for the BaO-Al_2O_3 system. While for the BaO-SiO_2 system, it was observed that associate model can better reproduce the experimental data than the substitutional solution model, especially for the reproduction of the liquidus in the SiO_2-rich region. The test of applying two associates to model the liquid phase in the BaO-SiO_2 systems was conducted, leading to the result of slightly improved description of the liquidus. A good fit with the literature data was achieved for the SrO-SiO_2 system by associate solution model to illustrate the liquid phase. According to the calculated site fractions of various species in the molten phase of BaO-SiO_2 and SrO-SiO_2 systems (Figure 17), the dominations of the associates can be obviously observed, indicating a strong short range order in the liquid phase. Although the existence of the associates in the silicate system was referred in some work, it should be pointed out that the domination of the associates in the present work is calculated based on the mathematical expression of the Gibbs energy functions, instead of being experimentally confirmed.

6.3 Future work

The thesis contains the experimental and thermodynamic investigation concerning the basic binary systems of the BaO-SrO-CaO-MgO-Al_2O_3-SiO_2 system. The study should be extended to higher order systems in the future to facilitate the establishment of the complete thermodynamic database applied in the industrial processes.

The study on the phase stabilities of the stoichiometric compounds below 1473K in the oxides systems can be made to acquire the experimental data in a wider temperature range. Due to the poor availability of the information for the ternary oxides systems, more focus should be paid on the expansion of the knowledge base on the isothermal sections, isopleths and thermodynamic properties of the ternary systems by using various experimental techniques. It not only contributes to provide more experimental data for extrapolation and thermodynamic modelling of the ternary system, but improves the understanding of phase equilibria and chemical processes in the industrial applications, such as, solid oxide fuel cell (SOFC) based on the BaO-Al_2O_3-SiO_2

system, removal of boron and phosphorous by using Al_2O_3-CaO-MgO-SiO_2 slag or BaO-Al_2O_3-SiO_2 slag and low temperature co-fired ceramics and so on.

The feasibility of the associate solution model remains to be tested with more oxides systems outside this thesis. Despite the capability of well reproducing the experimental data by using associate solution model, the development of thermodynamic model with physical meaning should be paid more attentions. This not only ensures that the thermodynamic modelling is performed based on the physical grounds but eases the extrapolation towards higher orders with high accuracy and reliability.

References

1. J. Chipman, Chemical behaviour of sulphur in iron and steelmaking. Metals Progress. 62 (1952) 97-107.
2. J. Chipman, L. Chang, The ionic nature of metallurgical slags – simple oxide systems. Transactions of the Metallurgical Society of AIME. 185 (1949) 191-197.
3. G.S. Powley, T.P. Floridis, Effect of barium oxide on the desulfurizing capacity of slags. Metallurgical Transactions. 1 (1970) 311-313.
4. R.E. Boni, G. Derge, Surface structure of non-oxidizing slags containing sulphur. Transactions of the Metallurgical Society of AIME. 206 (1956) 58-64.
5. J. Ma, Study and analysis on the desulfurization function of BaO and CaO in molten steel. Shanghai Metals. 1 (1998) 11.
6. F. Heydari, A. Maghsoudipour, Z. Hamnabard, S. Farhangdoust, Evaluation on properties of CaO-BaO-B_2O_3-Al_2O_3-SiO_2 glass-ceramic sealants for intermediate temperature solid oxide fuel cells. Journal of Materials Science and Technology. 29 (2013) 49-54.
7. M.K. Mahapatra, K. Lu. Seal glass for solid fuel cells. Journal of Power Sources. 195 (2010) 7129-7139.
8. A.A. Reddy, D.U. Tulyaganov, M.J. Pascual, V.V. Kharton, E.V. Tsipis, V.A. Kolotygin, J.M.F. Ferreira, Diopside-Ba disilicate glass-ceramic sealants for SOFCs: Enhanced adhesion and thermal stability by Sr for Ca substitution. International Journal of Hydrogen Energy. 38 (2013) 3073-3086.
9. R.R. Tummala, Ceramic and glass-ceramic packaging in the 1990s. Journal of the American Ceramic Society. 74 (1991) 895-908.
10. M.T. Sebastian, H. Jantunen, Low loss dielectric materials for LTCC applications: a review. 53 (2008) 57-90.
11. B. Li, B. Tang, M.J. Xu, Influences of CaO on crystallisation, microstructures and properties of BaO-Al2O3-B2O3-SiO2 glass-ceramics. Journal of electronic materials. 44 (2015) 3849-3854.
12. J.J.V. Laar, Melting or solidification curves in binary system. Zeitschrift für Physikalische Chemie. 63 (1908) 216.
13. J.J.V. Laar, Melting or solidification curves in binary system, part II. Zeitschrift für Physikalische Chemie. 64 (1908) 257-297

14. L. Kaufman, The industrial use of thermochemical data. No. 34 in the proceedings on the Industrial Use of Thermochemical Data, ed. T.I. Barry. CRC Press (1980).
15. H.L. Lukas, S.G. Fries, B. Sundman, Computational thermodynamics- the Calphad method. Cambridge, UK: Cambridge University Press (2007).
16. M. Hillert, B. Jansson, B. Sundman, J. Årgen, A two-sublattice model for molten solutions with different tendency for ionization. Metallurgical Transactions A. 16 (1985) 261-266.
17. B. Sundman. Modification of the two-sublattice model for liquids. CALPHAD. 15 (1991) 109-119.
18. P.L. Lin, A.D. Pelton, A structural model for binary silicate systems. Metallurgical Transactions B. 10 (1979) 667-675.
19. F. Sommer, Association model for the description of the thermodynamic functions of liquid alloys. Zeitschrift für Metallkunde. 73 (1982) 72-76.
20. H.G. Krull, R.N. Singh, F. Sommer, Generalised association model. Zeitschrift für Metallkunde. 91 (2000) 356-365.
21. M.L. Kapoor, G.M. Frohber, Proc. Sym., Sheffield, ISI London (1971) 17.
22. R.G. Berman, T.H. Brown, A thermodynamic model for multicomponent metls, with application to the system CaO-Al_2O_3-SiO_2. Geochimica et Cosmochimica Acta. 58 (1984) 661-678.
23. J.O. Andersson, T. Helander, L. Höglund, P.F. Shi, B. Sundman, Thermo-Calc and DICTRA, Computational tools for materials science. CALPHAD. 26 (2002) 273.312.
24. MTOX oxide database, Release Notes for Version 8.1 of Mtox Database, National Physical Laboratory, Teddington, UK, (2015).
25. R.H. Davies, A.T. Dinsdale, J.A. Gisby, J.A.J. Robinson, S.M. Martin, CALPHAD. 26 (2002) 229-271.
26. N. Sauders, A.P. Miodownik, CALPHAD, calculation of phase diagrams. R.W. Cahn (Ed.), Pergamon Materials Series (1998).
27. L. Kaufman, H. Berstein, Computer calculation of phase diagrams. With special reference to refractory metals. Academic Press Inc, New York. 4 (1970) 344.
28. H.H. Mao, Thermodynamic modelling and assessment of some alumino-silicate systems. Doctoral Dissertation, Royal Institute of Technology, Sweden (2005).
29. S.L. Chen, F. Zhang, Y. Xie, S. Daniel, X.Y. Yan, Y.A. Chang, R.C. Fetzer, W.A. Oates, Calculating phase diagrams using PANDATA and panengine. The Journal of Minerals, Metals and Materials Society. 55 (2003) 48-51.
30. Z.K. Liu. First-principles calculations and CALPHAD modelling of thermodynamics. Journal of Phase Equilibria and Diffusion. 30 (2009) 517-534.
31. A.A. Luo, W. Sun, W. Zhong, J.C. Zhao, Computational thermodynamics and kinetics for magnesium alloy development. Advanced Materials and Processes. 173 (2015) 26-30.

32. J. Allison, D. Backman, L. Christodoulou, Integrated computational materials engineering: A new paradigm for the global materials profession. The Journal of Minerals, Metals and Materials Society. 58 (2006) 25-27.
33. J. Allison, M. Li, C. Wolverton, X.M. Su, Virtual aluminum castings: An industrial application of ICME. The Journal of Minerals, Metals and Materials Society. 58 (2006) 28-35.
34. D. Apelian, Integrated computational materials engineering (ICME): A 'model' for the future. The Journal of Minerals, Metals and Materials Society. 60 (2008) 9-10.
35. J. Allison, Integrated computational materials engineering: A perspective on progress and future steps. The Journal of Minerals, Metals and Materials Society. 63 (2011) 15-18.
36. A.A. Luo, Material design and development: From classical thermodynamics to CALPHAD and ICME approaches. CALPHAD. 50 (2015) 6-22.
37. The SGTE Substance Database, SGTE (Scientific Group Thermodata Europe), Grenoble, France (1994).
38. H.H. Mao, M. Selleby, B. Sundman, A re-evaluation of the liquid phases in the CaO-Al_2O_3 and MgO-Al_2O_3 systems. Calphad, 28 (2004) 307-312.
39. H.H. Mao, M. Selleby, O. Fabrichnaya, Themodynamic reassessment of the Y_2O_3-Al_2O_3-SiO_2 system and its subsystems. Calphad. 32 (2008) 399-412.
40. B. Hallstedt, Assessment of the CaO-Al_2O_3 system. Journal of the American Ceramic Society. 73 (1990) 15-23.
41. B Hallstedt, Thermodynamic assessment of the system MgO-Al_2O_3. Journal of the American Ceramic Society. 75 (1992) 1497-1507.
42. M. Hillert, The compound energy formalism. Journal of Alloys and Compounds. 320 (2001) 161-176.
43. K. Frisk, M. Selleby, The compound energy formalism: applications. Journal of Alloys and Compounds 320 (2001) 177-188.
44. O. Redlich, A. Kister, Thermodynamics of nonelectrolytic solutions, algebraic representation of thermodynamic properties and classification of solutions. Industrial and Engineering Chemistry. 40 (1948) 345-348.
45. H. Kopp, Investigations of the specific heat of solid bodies. Philosophical Transactions. 155 (1865) 71-202.
46. J. Leitner, P. Voňka, D. Sedmidubsky, P. Svoboda, Application of Neumann-Kopp rule for the estimation of heat capacity of mixed oxides. Thermochimica Acta. 497 (2010) 7-13.
47. J. Leitner, P. Chuchvalec, D. Sedmidubsky, A. Strejc, P. Abrman, Estimation of heat capacities of solid mixed oxides. Thermochimica Acta. 395 (2002) 27-46.
48. L. Qiu, M.A. White, The constituent additivity method to estimate heat capacities of complex inorganic solids. Journal of Chemical Education. 78 (2001) 1076-1079.
49. M. Selleby, Thermodynamic modelling and evaluation of the Ca-Fe-O-Si system. Doctoral Dissertation, Royal Institute of Technology, Sweden (1993).

50. Thermo-Calc Data Optimisation User Guide, Version 2015a. 1995-2015 Foundation of Computational Thermodynamics Stockholm, Sweden.
51. Methods for phase diagram determination (Ed. J.C. Zhao). Elsevier (2007).
52. E.E. Schumacher, Melting points of barium, strontium and calcium oxides. Journal of the American Chemical Society. 48 (1926) 396-402.
53. J.J. Lander, The phase system BaO-$BaCO_3$. Journal of American Chemical Society. 73 (1951) 5893-5894.
54. E.H. Baker, The barium oxide-carbon dioxide system in the pressure range 0.01-450 atmospheres. Journal of the Chemical Society. 137 (1964) 699-704.
55. E.M. Levin, H.F. McMurdie, The system BaO-B_2O_3. Journal of the American Ceramic Society. 32 (1949) 100.
56. S.J. Schneider, C.L. McDaniel, The BaO-Pt system in air. Journal of the American Ceramic Society. 52 (1969) 518-519.
57. P.K. Gallagher, D.W. Johnson, E.M. Vogel, G.K. Wertheim, F.J. Schnettler, Synthesis and structure of BaPtO3. Journal of Solid State Chemistry. 21 (1977) 277-282.
58. R. Zhang, P. Taskinen, A thermodynamic assessment of the BaO-MgO, BaO-CaO, BaO-Al_2O_3 and BaO-SiO_2 systems. Aalto University Publication Series SCIENCE+TECHNOLOGY, Finland (2014).
59. H.V. Wartenberg, E. Prophet, Melting diagrams of maximum fireproof oxides. V. Systems with MgO. Zeitschrift für Anorganische und Allgemeine Chemie. 208 (1932) 369-379.
60. W.J.M. Van-der Kemp, J.G. Blok, P.R. Van-der Linde, H.A.J. Oonk, A. Schuijff, Binary alkaline earth oxide mixtures: estimation of the excess thermodynamic properties and calculation of the phase diagrams. Calphad. 18 (1994) 255-267.
61. A. Shukla, Development of a critically evaluated thermodynamic database for the systems containing alkaline-earth oxides. Doctoral Dissertation. Ecole Polytechnique de Montreal, Canada (2012).
62. R.N. Macnally, F.I. Peters, P.H. Ribbe, Laboratory furnace for studies in controlled atmospheres; melting points of MgO in a N2 atmosphere and of Cr_2O_3 in N_2 and in air atmospheres. Journal of the American Ceramic Society. 44 (1961) 491.
63. S.J. Schneider, Compilation of the melting points of the metal oxides - Technical Report, National Bureau of Standards, Washington, D.C., monograph, number 68 (1963).
64. C. Ronchi, M. Sheindlin, Melting point of MgO. Journal of Applied Physics. 90 (2001) 3325-3331.
65. G.V. Flidlider, T.V. Kovtunenko, E.V. Kiseleva, A.A. Bundel, The relation between the heats of formation of solid solutions of alkaline earth metal oxides and their capacity for thermionic emission. Russian Journal of Physical Chemistry. 40 (1966) 1329-1331.
66. W.G. Seo, D.H. Zhou, F. Tsukihashi, Calculation of thermodynamic properties and phase diagrams for the CaO-CaF2, BaO-CaO and BaO-CaF2

systems by molecular dynamics simulation, Mater. Trans. 46 (2005) 643-650.
67. W.J.M. Van Der Kemp, H.A.J. Oonk, Determination of the excess molar Gibbs energy of (1-x) BaO+x SrO by means of Knudsen-effusion mass spectrometry. Journal of Chemical Thermodynamics. 24 (1992) 857-862.
68. K.T. Jacob, V. Varghese, Solid-state miscibility gap and thermodynamic of the system BaO-SrO. Journal of Materials Chemistry. 5 (1995) 1059-1062.
69. P. Appendino, Research on the Most Basic Area of the $BaO-Al_2O_3$ system. Annali Di Chimica. 61 (1971) 822-830.
70. G. Purt, Binary system of $BaO-Al_2O_3$, Radex Rundschau. 4 (1960) 198-202.
71. N.A. Toropov, F.Y. Galakhov, Phase Diagram of the $BaO-Al_2O_3$ System. Doklady Akademii Nauk SSSR. 82 (1952) 69-70.
72. L.M. Kovba, L.N. Lykova, E.V. Antipov, M.V. Paromova, O.N. Rozanova, Double Oxides of Barium and Aluminum. Russian Journal of Inorganic Chemistry. 32 (1987) 301-302.
73. P. Eskola, The silicates of strontium and barium. American Journal of Science. 4 (1922) 343-375.
74. E.M. Levin, G.M. Ugrinic, The system barium oxide-boric oxide-silica. Journal of Research of the National Bureau of Standards. 62 (1959) 193-200.
75. G. Oehlschlegel, The binary partial system $BaO_2{\cdot}SiO_2$-$2BaO{\cdot}3SiO_2$. Glastechnische Berichte. 44 (1971) 194-204.
76. G. Oehlschlegel, Crystallization of glasses in the system $BaO_2{\cdot}SiO_2$-$2BaO{\cdot}3SiO_2$. Journal of the American Ceramic Society. 58 (1975) 148-149.
77. J.W. Greig, Immiscibility in silicate melts. American Journal of Science. 13 (1927) 1-44.
78. Ol'shanskij, Equilibrium of two immiscible liquids in silicate systems of alkali-earth metals, Doklady Akademii Nauk SSSR. 76 (1951) 93-96.
79. F.C. Kracek, The cristobalite liquidus in the alkali oxide-silica systems and the heat of fusion of cristobalite. Journal of the American Chemical Society. 52 (1930) 1436-1442.
80. G.N. Shabanova, V.V. Taranenkova, A.N. Korogodskaya and E.V. Khristich, Structure of the $BaO-Al_2O_3-SiO_2$ system (A review). Glass Ceramics. 60 (2003) 43-46.
81. R. Zhang; P. Taskinen, Phase equilibria investigation in the $BaO-SiO_2-Al_2O_3$ ternary system at 1500 °C. Key Engineering Materials. 697 (2016) 565-571. Trans Tech Publications, Switzerland.

Knowledge of the phase equilibria and thermodynamic properties is significant to understand the microstructure and properties of the materials based on BaO-containing system. By employing experimental investigation, with assistance of the CALPHAD (CALculation of PHAse Diagram) technique, it is possible to establish a thermodynamic database capable of describing the complex oxide system, in a way to model and predict the phase equilibria, thermodynamic properties and chemical process of the desired systems.

Based on (i) high-temperature equilibration/quenching technique coupled with SEM/EDS, EPMA and XRD analysis, and (ii) thermodynamic modelling using Thermo-Calc, the present work successfully investigated six binary systems and one ternary system. The phase equilibria data and thermodynamic properties were digitalized into thermodynamic database in the format of Gibbs energy functions.

ISBN 978-952-60-6935-7 (printed)
ISBN 978-952-60-6934-0 (pdf)
ISSN-L 1799-4934
ISSN 1799-4934 (printed)
ISSN 1799-4942 (pdf)

Aalto University
School of Chemical Technology
Department of Materials Science and Engineering
www.aalto.fi

BUSINESS + ECONOMY

ART + DESIGN + ARCHITECTURE

SCIENCE + TECHNOLOGY

CROSSOVER

DOCTORAL DISSERTATIONS

Aalto-DD 148/2016